

Computer Assisted Proof for Normally Hyperbolic Invariant Manifolds

Maciej J. Capiński

Faculty of Applied Mathematics, AGH University of Science and Technology,
Mickiewicza 30, 30-059 Kraków, Poland

E-mail: mcapinsk@agh.edu.pl

Carles Simó

Departament de Matemàtica Aplicada i Anàlisi, Universitat de Barcelona, Gran Via
585, 08007 Barcelona, Spain

E-mail: carles@maia.ub.es

Abstract. We present a topological proof of the existence of a normally hyperbolic invariant manifold for maps. In our approach we do not require that the map is a perturbation of some other map for which we already have an invariant manifold. But a non-rigorous, good enough, guess is necessary. The required assumptions are formulated in a way which allows for an “a posteriori” verification by rigorous-interval-based numerical analysis. We apply our method for a driven logistic map, for which non-rigorous numerical simulation in plain double precision suggests the existence of a chaotic attractor. We prove that this numerical evidence is false and that the attractor is a normally hyperbolic invariant curve.

1. Introduction

In this paper we give a proof of existence of normally hyperbolic invariant manifolds for maps. The construction is performed in the state space of the map. Assumptions needed for the proof are of twofold nature. First we require topological conditions which follow from suitable alignment of the coordinates (these are the so called covering relations). Next we require that our map satisfies cone conditions. The aim of the paper though is not to produce yet another proof of the normally hyperbolic invariant manifold theorem. Our aim is to produce a tool that can be applied in rigorous-computer-assisted proofs.

To show the strength of our approach we apply our theorem to a driven logistic map introduced in [2]. The map considered is such that standard numerical simulation gives evidence of a chaotic attractor. Nevertheless we will show that the map in fact possesses a normally hyperbolic invariant curve. This is apparent also when simulations are performed using multiple precision computations. The example is a demonstration of the fact that one has to be careful with the arithmetics in simulations, since the numerical evidence of an attractor is false. See, e.g., [11] and [19] for other similar examples. The strength of our method lies in the fact that even for such a simple example as the one in [2], which defeats standard numerical simulations, we are able to produce a rigorous proof of existence of a normally hyperbolic invariant curve.

The approach to normally hyperbolic manifolds presented here is in the spirit of [3] and [6]. In [3] a topological proof of existence of invariant sets with normally hyperbolic type properties is given. In [6] the result is extended to prove existence of normally hyperbolic invariant manifolds. In both cases the proofs relied on assumptions that the first iterate of the map is well aligned with the stable and unstable manifolds. Similar approach was also used in [4] to give a proof of existence of a center manifold. The result in [4] is for ODEs and relies also on the fact that hyperbolic dynamics is uniform. The main difference between our paper and the results mentioned above is that we assume that hyperbolic expansion and contraction aligns with the tangent spaces of the invariant manifolds after a suitable (possibly large) number of iterates of the map. This setting is more general, and also more typical for normal hyperbolicity.

The paper is organised as follows. Section 2 introduces basic notations used throughout the paper and provides a setup and an outline of our argument. Section 3 contains a geometric construction of a normally hyperbolic manifold. We first give a construction of a “center-stable” manifold (the term “center-stable” refers to the normally hyperbolic invariant manifold union its associated stable manifold; analogous terminology is used by us for the “center-unstable” manifold). A center-unstable manifold is obtained using a mirror construction to the center-unstable manifold, by considering the inverse map. The intersection of the center-stable and center-unstable manifolds gives us the normally hyperbolic invariant manifold. In Section 4 we show how to verify the assumptions of our theorems using local bounds on derivatives of the map. In Section 5 we present our example of the driven logistic map and apply our method to it.

2. Setup

We start by writing out some basic notations which we shall use throughout the paper. A notation $B_i(q, r)$ will stand for a ball of radius r centered at q in \mathbb{R}^i . We will also use the notation $B_i = B_i(0, 1)$. For a set A we will denote by \overline{A} its closure, by $\text{int } A$ its interior and by ∂A its boundary. For a function f we will use the notation $\text{dom}(f)$ to denote its domain. For points $p = (x, y)$ we shall use the notation $\pi_x(p)$, $\pi_y(p)$ to denote the projection onto the x and y coordinates respectively.

We now introduce the setup of our problem. Let D and \mathcal{U} be open subsets in \mathbb{R}^n such that $D \subset \mathcal{U}$. Let

$$f : \mathcal{U} \rightarrow \mathcal{U},$$

be a diffeomorphism. Let $u, s, c \in \mathbb{N}$ be such that $u + s + c = n$. We assume that there exist a diffeomorphism

$$\phi : \mathcal{U} \rightarrow \phi(\mathcal{U}) \subset \mathbb{R}^u \times \mathbb{R}^s \times \Lambda$$

such that $\phi(\overline{D}) = D_\phi := \overline{B}_u \times \overline{B}_s \times \Lambda$, and Λ is a compact c dimensional manifold without boundary. We define $f_\phi : D_\phi \rightarrow \mathbb{R}^u \times \mathbb{R}^s \times \Lambda$ as

$$f_\phi = \phi \circ f \circ \phi^{-1}.$$

We assume that there exists a finite covering $\{U_i\}_{i \in I}$ of Λ and an atlas

$$\eta_i : \overline{U}_i \rightarrow \overline{B}_c.$$

Throughout the work we will use the notation

$$\mathbf{B} = \overline{B}_u \times \overline{B}_s \times \overline{B}_c.$$

For $i, j \in I$ we consider local maps $f_{ji} : \mathbf{B} \supset \text{dom}(f_{ji}) \rightarrow \mathbb{R}^u \times \mathbb{R}^s \times \overline{B}_c$ defined as

$$\begin{aligned} f_{ij} &:= \tilde{\eta}_j \circ f_\phi \circ \tilde{\eta}_i^{-1}, \\ \tilde{\eta}_i &:= (\text{id}, \text{id}, \eta_i) \quad \text{for } i \in I. \end{aligned}$$

Note that the domain of f_{ij} can be empty, and will usually be smaller than \mathbf{B} . The following graph depicts the functions defined above and their mutual relations.

$$\begin{array}{ccc} D & \xrightarrow{f} & \mathcal{U} \\ \downarrow \phi & & \downarrow \phi \\ \overline{B}_u \times \overline{B}_s \times \Lambda & \xrightarrow{f_\phi} & \mathbb{R}^u \times \mathbb{R}^s \times \Lambda \\ \downarrow \tilde{\eta}_i & & \downarrow \tilde{\eta}_j \\ \mathbf{B} & \xrightarrow{f_{ji}} & \mathbb{R}^u \times \mathbb{R}^s \times \overline{B}_c \end{array}$$

Our goal in this paper will be to find a normally hyperbolic invariant manifold, together with its stable and unstable manifolds within the set D , provided we have some numerically verifiable conditions.

We will use the following notations for our coordinates: $x \in \mathbb{R}^u$, $y \in \mathbb{R}^s$, $\theta \in \overline{B}_c$, $\lambda \in \Lambda$. The coordinate x will play the role of a globally unstable direction, and the

coordinate y will play the role of a stable direction for the map f_ϕ (hence the superscripts u and s , which stand for “unstable” and “stable” respectively). The coordinate λ will play the role of the central direction, which globally has weaker contraction than in the stable coordinate, and weaker expansion than in the unstable one. The notation θ will also be used for the central direction, but it will be reserved to denote the central coordinate in the local coordinates; i.e. $\theta = \eta_i(\lambda)$ for some $\lambda \in \Lambda$ and $i \in I$.

3. Geometric approach to invariant manifolds

In this section we give the construction of a normally hyperbolic invariant manifold. The construction is performed in the state space of our map. It is based on the assumptions of covering relations and cone conditions. We first give an introduction to these tools in Section 3.1. In Section 3.2 we formulate our assumptions on the map in terms of covering relations and cone conditions, which will imply the existence of a normally hyperbolic manifold. In Section 3.3 we show how to construct a center-stable manifold of our map. The construction of a center-unstable manifold follows from a mirror argument. The intersection of center-stable and center-unstable manifolds gives us a C^0 normally hyperbolic invariant manifold. Let us write explicitly that for a normally hyperbolic manifold which does not have an associated stable manifold, the center-stable manifold will be the normally hyperbolic manifold itself. An analogous statement holds also for center-unstable manifolds.

3.1. Covering relations and cones

Covering relations are topological tools used for proofs of nontrivial symbolic dynamics of dynamical systems. The method is based on the Brouwer degree theory, and the setting is such that it allows for rigorous numerical verification. The method has been applied in computer assisted proofs of existence of chaotic dynamics for the Hénon map, Rössler equations [22], [6], Lorenz equations [8], Chua circuit [7] or for the solitons in the Kuramoto-Sivashinsky PDE [21], amongst others. The method is based on singling out a number of regions, called h-sets, which have hyperbolic type properties. Using these properties one can find orbits of the system, which shadow the h-sets along their trajectories. The method of covering relations relies on the system having expanding and contracting coordinates. In this section we generalize covering relations to include also a central direction. The setup is similar to that of [3], [5], but has been simplified. Our proofs are now simpler and based only on continuity arguments. They no longer require the use of degree theory, with little loss of generality.

For any $p = (x, y, \theta) \in \mathbf{B}$ and $r_u, r_s, r_c > 0$ we introduce a notation

$$N(p, r_u, r_s, r_c) := \overline{B}_u(x, r_u) \times \overline{B}_s(y, r_s) \times \overline{B}_c(\theta, r_c).$$

We define

$$N^- = N^-(p, r_u, r_s, r_c) := \partial \overline{B}_u(x, r_u) \times \overline{B}_s(y, r_s) \times \overline{B}_c(\theta, r_c),$$

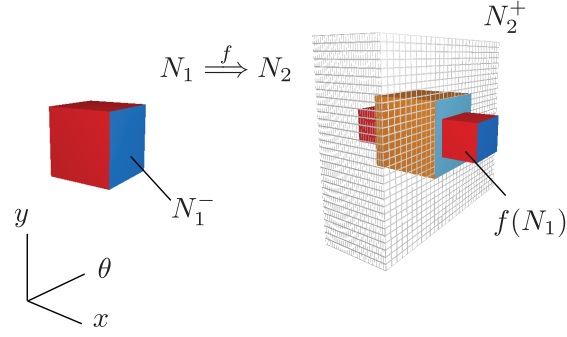


Figure 1. A ch-set N_1 covering a ch-set N_2 .

$$\begin{aligned} N^+ &= N^+(p, r_u, r_s, r_c) \\ &:= \overline{B}_u(x, r_u) \times ((\mathbb{R}^s \times \mathbb{R}^c) \setminus (B_s(y, r_s) \times B_c(\theta, r_c))). \end{aligned}$$

We assume that all boxes N which we are going to consider here are contained in \mathbf{B} . We will refer to a box N as a *ch-set* (center-hyperbolic set) centered at p .

In the following arguments we shall often consider different ch-sets. To keep better track of our notations and to make our arguments more transparent we will stick to the convention that for two ch-sets N_1, N_2 centered respectively at $p_1 = (x_1, y_1, \theta_1)$ and $p_2 = (x_2, y_2, \theta_2)$ we write

$$N_i = N_i(p_i, r_u^i, r_s^i, r_c^i) := \overline{B}_u^i(x_i, r_u^i) \times \overline{B}_s^i(y_i, r_s^i) \times \overline{B}_c^i(\theta_i, r_c^i) \quad \text{for } i = 1, 2.$$

Definition 1. Let $g : \mathbf{B} \rightarrow \mathbb{R}^u \times \mathbb{R}^s \times \overline{B}_c$ be a continuous function. Let $p_i = (x_i, y_i, \theta_i)$ for $i = 1, 2$ and let N_1, N_2 be two ch-sets in \mathbf{B} centered at p_1 and p_2 respectively. We say that N_1 g -covers N_2 if

$$g(p_1) \in \text{int}(N_2), \tag{1}$$

$$\pi_x(g(N_1^-)) \cap \overline{B}_u^2(x_2, r_u^2) = \emptyset, \tag{2}$$

$$g(N_1) \cap N_2^+ = \emptyset. \tag{3}$$

In such case we shall write $N_1 \xrightarrow{g} N_2$.

Remark 2. Definition 1 is a simplified definition of a covering relation. More general versions can be found in [8], [9], [22] in the setting of hyperbolicity, or in [3], [5] in a setting when additionally a central direction is included.

For $\gamma = (a, b, c) \in \mathbb{R}^3$, and $q = (x, y, \theta) \in \mathbb{R}^u \times \mathbb{R}^s \times \mathbb{R}^c$ we define

$$\begin{aligned} Q_\gamma &: \mathbb{R}^u \times \mathbb{R}^s \times \mathbb{R}^c \rightarrow \mathbb{R}, \\ Q_\gamma(q) &:= a \|x\|^2 + b \|y\|^2 + c \|\theta\|^2. \end{aligned} \tag{4}$$

If $a > 0, b, c < 0$, then for $p \in \mathbb{R}^u \times \mathbb{R}^s \times \mathbb{R}^c$ we will refer to

$$C(p, \gamma) := \{q : Q_\gamma(p - q) \geq 0\}$$

as a *horizontal cone* centered at p (see Figure 2).

Definition 3. Let N be a ch-set and $\gamma = (a, b, c)$ be such that $a > 0$, $b, c < 0$. We will refer to a pair (N, γ) as a ch-set with cones.

Definition 4. Let $(N, \gamma) = (N((x, y, \theta), r_u, r_s, r_c), \gamma)$ be a ch-set with cones. A continuous function $\mathbf{h} : \overline{B}_u(x, r_u) \rightarrow N$ is called a horizontal disc in (N, γ) , iff $\pi_x \mathbf{h}(x) = x$ and for any $x^*, x^{**} \in \overline{B}_u(x, r_u)$,

$$Q_\gamma(\mathbf{h}(x^*) - \mathbf{h}(x^{**})) \geq 0, \quad (5)$$

Lemma 5. Let $N_i = N_i((x_i, y_i, \theta_i), r_u^i, r_s^i, r_c^i)$ for $i = 1, 2$ and let (N_1, γ_1) , (N_2, γ_2) be two ch-sets with cones. Assume that

$$N_1 \xrightarrow{g} N_2 \quad (6)$$

and that for any $q^*, q^{**} \in N_1$ such that $q^* \neq q^{**}$ and $Q_{\gamma_1}(q^* - q^{**}) \geq 0$ we have

$$Q_{\gamma_2}(g(q^*) - g(q^{**})) > 0. \quad (7)$$

If \mathbf{h}_1 is a horizontal disc in (N_1, γ_1) then there exists a horizontal disc \mathbf{h}_2 in (N_2, γ_2) such that $g(\mathbf{h}_1(\overline{B}_u^1(x_1, r_u^1))) \cap N_2 = \mathbf{h}_2(\overline{B}_u^2(x_2, r_u^2))$.

Proof. Without loss of generality we assume that $p_1 = p_2 = 0$ and that $r_\kappa^i = 1$ for $i = 1, 2$ and $\kappa \in \{u, s, c\}$. In other words, we assume that for $i = 1, 2$

$$N_i = \overline{B}_u^i \times \overline{B}_s^i \times \overline{B}_c^i = \overline{B}_u(0, 1) \times \overline{B}_s(0, 1) \times \overline{B}_c(0, 1).$$

Let $\gamma_i = (a_i, b_i, c_i)$ for $i = 1, 2$ and let \mathbf{h} be any horizontal disc in N_1 . Then by (4), (5) and (7) for $x^*, x^{**} \in \overline{B}_u^1$, $x^* \neq x^{**}$

$$a_2 \|\pi_x g(\mathbf{h}(x^*)) - \pi_x g(\mathbf{h}(x^{**}))\|^2 \geq Q_{\gamma_2}(g(\mathbf{h}(x^*)) - g(\mathbf{h}(x^{**}))) > 0, \quad (8)$$

which means that $\pi_x \circ g \circ \mathbf{h}$ is injective.

Using the notation $\mathbf{h}_1(x) = (x, h_1(x)) \in \overline{B}_u^i \times (\overline{B}_s^i \times \overline{B}_c^i)$, for $\alpha \in [0, 1]$, we define a family of horizontal discs $\mathbf{h}_\alpha(x) = (x, \alpha h_1(x))$. Let $F_\alpha : \overline{B}_u^1 \rightarrow \mathbb{R}^u$ be a continuous family of functions defined as

$$F_\alpha(x) := \pi_x \circ g \circ \mathbf{h}_\alpha(x).$$

We shall show that $\overline{B}_u^2 \subset F_1(B_u^1)$. Functions F_α are injective, hence sets $A_\alpha := F_\alpha(B_u^1)$ are homeomorphic to balls in \mathbb{R}^u ; moreover $\partial A_\alpha = F_\alpha(\partial B_u^1)$. By Definition 4 of a horizontal disc, $\mathbf{h}_\alpha(\partial B_u^1) \subset N_1^-$. From assumption (6), by conditions (1), (2) we have:

$$\pi_x g(0) \in \overline{B}_u^2, \quad (9)$$

$$\partial A_\alpha \cap \overline{B}_u^2 \subset F_\alpha(N_1^-) \cap \overline{B}_u^2 = \emptyset. \quad (10)$$

From the fact that $0 \in B_u^1$ we have:

$$F_0(0) \in F_0(B_u^1) = A_0. \quad (11)$$

Since $\mathbf{h}_0(0) = 0$, by (9) we have:

$$F_0(0) = \pi_x \circ g \circ \mathbf{h}_0(0) = \pi_x g(0) \in \overline{B}_u^2. \quad (12)$$

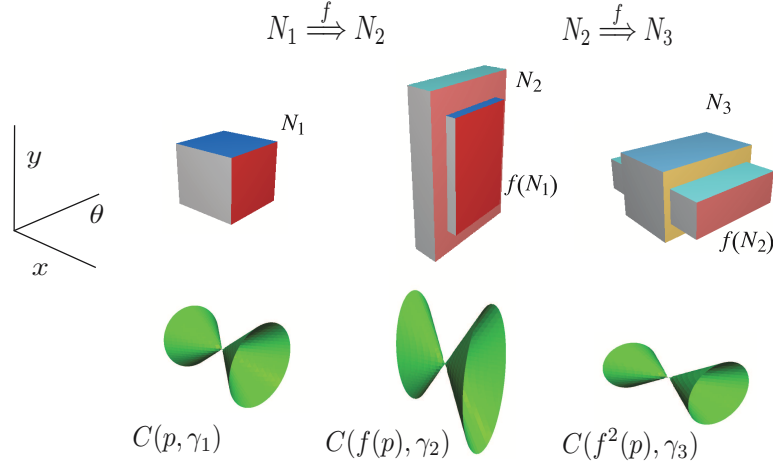


Figure 2. Covering relations for two iterates of a map f . For the second iterate of the map the coordinate x is expanding and y is contracting (for the first iterate of f they are not). The fact that expansion in x is stronger than expansion in θ is visible from the fact that the cones $C(f^2(p), \gamma_3)$ are "tighter" than cones $C(p, \gamma_1)$.

From (11), (12) it follows that $A_0 \cap \overline{B}_u^2 \neq \emptyset$. This by (10) implies that $\overline{B}_u^2 \subset A_0$. By continuity of F_α with respect to α this means that $\overline{B}_u^2 \subset A_\alpha$ for all $\alpha \in [0, 1]$. In particular $\overline{B}_u^2 \subset A_1 = F_1(B_u^1)$.

Since F_1 is injective and $\overline{B}_u^2 \subset F_1(B_u^1)$, for any $v \in \overline{B}_u^2$ there exists a unique $x = x(v) \in B_u^1$ such that $F_1(x) = v$. We define $\mathbf{h}_2(v) = (v, h_2(v)) := (v, \pi_{y,\theta} \circ g \circ \mathbf{h}_1(x(v)))$. For any $v^* \neq v^{**}$, $v^*, v^{**} \in \overline{B}_u^2$, by (5) and (7) we have

$$\begin{aligned} Q_{\gamma_2}(\mathbf{h}_2(v^*) - \mathbf{h}_2(v^{**})) &= Q_{\gamma_2}(g \circ \mathbf{h}_1(x(v^*)) - g \circ \mathbf{h}_1(x(v^{**}))) \\ &> Q_{\gamma_1}(\mathbf{h}_1(x(v^*)) - \mathbf{h}_1(x(v^{**}))) \\ &> 0. \end{aligned}$$

Since $Q_{\gamma_2}(\mathbf{h}_2(v^*) - \mathbf{h}_2(v^{**})) > 0$ we have

$$\begin{aligned} a_2 \|v^* - v^{**}\| &> -b_2 \|\pi_y(h_2(v^*) - h_2(v^{**}))\|^2 - c_2 \|\pi_\theta(h_2(v^*) - h_2(v^{**}))\|^2 \\ &\geq \min(-b_2, -c_2) \|h_2(v^*) - h_2(v^{**})\|^2, \end{aligned}$$

and therefore \mathbf{h}_2 is continuous. \square

Remark 6. It is important to point out that since we have freedom of choice of the radii r_u, r_s and r_c it is not necessary for x to be expanding, y to be contracting and θ to have weaker dynamics for each single iterate of the map. In Figure 2 we have a sketch of a situation in which x becomes expanding and y contracting only after a second iterate. In Figure 2 the coordinate θ is expanding. It will turn out that such a scenario is acceptable for us and can be dealt with by increasing r_c for successive iterates.

3.2. Covering relations and cone conditions for normal hyperbolicity

In this section we formulate our assumptions which will imply the existence of a normally hyperbolic manifold. The assumptions are in terms of covering relations and cones and are in the spirit of [5]. There are two major differences though. The first is that the assumptions used in [5] required the system to have uniform expansion and uniform contraction for the first iterate of the map. Here we set up our coordinates in the directions of *global* contraction and *global* expansion. In the setting of normal hyperbolicity the coordinates of global contraction and expansion need not be contracting and expanding for the first iterates of the map. What is important is that they dominate after a sufficiently large numbers of iterates. In other words, that the Lyapunov exponents are negative or positive, respectively. We set up our assumptions so that they allow for such setting. This way we do not need to use the “adapted norms” to ensure that contraction/expansion happens in the first iterate. The second difference is that our setup has been significantly simplified with comparison to [5]. This results in a slight loss of generality (we do not formulate our assumptions in terms of vector bundles as in [5]) but we need to consider fewer assumptions.

Let $1 > R > \rho, r > 0$. Assume that there exists a finite sequence of points $\boldsymbol{\lambda}_k \in \Lambda$, $k \in \mathbb{N}$ such that for any k the set $I(k) = \{i : B_c(\eta_i(\boldsymbol{\lambda}_k), \rho) \subset B_c(0, R)\}$ is not empty. What is more, assume that there exists a set $J \subset \{(i, k) | i \in I(k)\}$ such that $\Lambda \subset \bigcup_{(i,k) \in J} \eta_i^{-1}(B_c(\eta_i(\boldsymbol{\lambda}_k), \rho))$. For points $(i, k) \in J$ we define sets

$$M_{i,k} := \overline{B}_u(0, r) \times \overline{B}_s(0, r) \times \overline{B}_c(\eta_i(\boldsymbol{\lambda}_k), \rho).$$

We will need to assume that the points $\boldsymbol{\lambda}_k$ are sufficiently close to each other. We will also need to assume that R and ρ are sufficiently large in comparison to r . This is summarized in Assumption 7. The idea behind it is demonstrated in Figure 3, which might provide some intuition.

Assumption 7. Let $\mathbf{m} > 1$ and let $\boldsymbol{\gamma}_0 = (\mathbf{a}_0, \mathbf{b}_0, \mathbf{c}_0) \in \mathbb{R}^3$, $\boldsymbol{\gamma}_1 = (\mathbf{a}_1, \mathbf{b}_1, \mathbf{c}_1) \in \mathbb{R}^3$ satisfy $\mathbf{a}_m > 0$, $\mathbf{b}_m, \mathbf{c}_m < 0$ for $m = 1, 2$. Let us also define a set $M \subset \mathbf{B}$ as

$$M := \overline{B}_u(0, r) \times \overline{B}_s(0, r) \times \overline{B}_c. \quad (13)$$

We assume that for any horizontal disc \mathbf{h} in a ch -set with cones $(M, \boldsymbol{\gamma}_1)$ and for any $i \in I$ there exists $(\iota, \kappa) \in J$ such that $\mathbf{h}(B_u(0, r)) \subset \text{dom}(\tilde{\eta}_\iota \circ \tilde{\eta}_i^{-1})$. In addition we assume that for any q^*, q^{**} in $\text{dom}(\tilde{\eta}_\iota \circ \tilde{\eta}_i^{-1})$ such that $Q_{\boldsymbol{\gamma}_1}(q^* - q^{**}) > 0$ we have

$$Q_{\boldsymbol{\gamma}_0}(\tilde{\eta}_\iota \circ \tilde{\eta}_i^{-1}(q^*) - \tilde{\eta}_\iota \circ \tilde{\eta}_i^{-1}(q^{**})) > \mathbf{m} Q_{\boldsymbol{\gamma}_1}(q^* - q^{**}) \quad (14)$$

and

$$\mathbf{h}' := \tilde{\eta}_\iota \circ \tilde{\eta}_i^{-1} \circ \mathbf{h}|_{B_u(0, r)} \quad \text{is a horizontal disc in } (M_{\iota, \kappa}, \boldsymbol{\gamma}_0). \quad (15)$$

Assumption 7 ensures that for \mathbf{h} in some local coordinates $\tilde{\eta}_i$ we can change to coordinates $\tilde{\eta}_\iota$ so that $\mathbf{h}' := \tilde{\eta}_\iota \circ \tilde{\eta}_i^{-1} \circ \mathbf{h}$ lies close to the middle of the set M . Assumption 7 is also discussed in Section 4.3, where conditions which imply it are given.

Above we use bold font for $\boldsymbol{\gamma}_i = (\mathbf{a}_i, \mathbf{b}_i, \mathbf{c}_i)$, $i = 0, 1$ to distinguish them from other $\boldsymbol{\gamma} = (a, b, c)$ in our proofs.

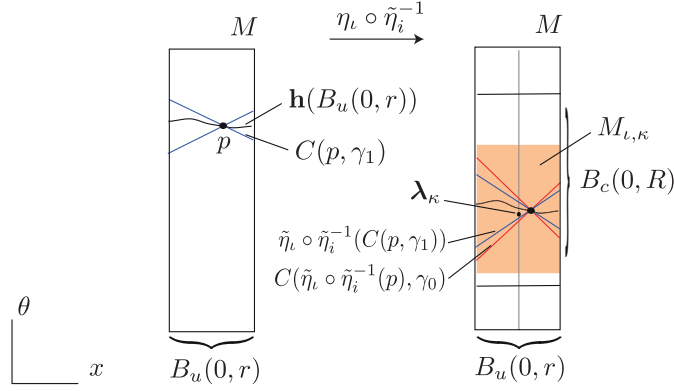


Figure 3. The change of coordinates $\tilde{\eta}_l \circ \tilde{\eta}_i^{-1}$, a horizontal disc \mathbf{h} , and the cones given by γ_0 and γ_1 in different local coordinates. Here, for simplicity, the stable coordinate is neglected $s = 0$.

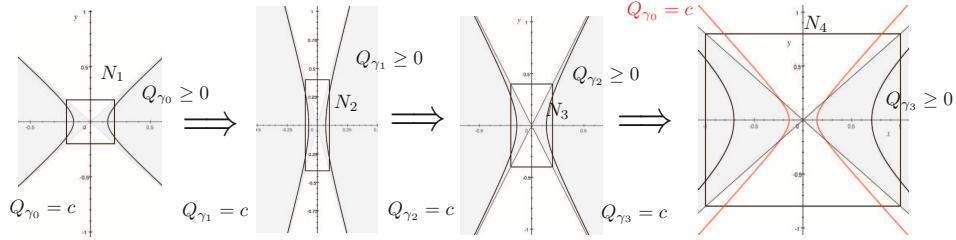


Figure 4. (see Example 9) For the first iterates of the map the ch-sets and cones are contracted in the x direction. After a number of steps the expansion in x starts to dominate. Note that the coordinate θ is expanding. Since expansion in x is stronger than expansion in θ though, the cones eventually become more flat and their level sets $Q_{\gamma_i} = c$ are pulled away from the origin.

Definition 8. If for any $(i, k) \in J$ there exists a sequence of ch-sets with cones $(N_1, \gamma_1), \dots, (N_n, \gamma_n)$ (n can depend on (i, k)) and a sequence $i_0 = i, i_1, \dots, i_n \in I$ such that

$$M_{i,k} =: N_0 \xrightarrow{f_{i_1 i_0}} N_1 \xrightarrow{f_{i_2 i_1}} N_2 \xrightarrow{f_{i_3 i_2}} \dots \xrightarrow{f_{i_n i_{n-1}}} N_n \xrightarrow{\text{id}} M, \quad (16)$$

then we say that f satisfies covering conditions.

If in addition for any $q_1, q_2 \in N_{l-1}$, $q_1 \neq q_2$,

$$Q_{\gamma_{l+1}}(f_{i_{l+1} i_l}(q_1) - f_{i_{l+1} i_l}(q_2)) > Q_{\gamma_l}(q_1 - q_2) \quad (17)$$

for $l = 0, \dots, n-1$, and for $\gamma_n = (a, b, c)$ we have

$$\mathbf{a}_1 > a, \quad \frac{\mathbf{b}_1}{\mathbf{a}_1} > \frac{b}{a}, \quad \frac{\mathbf{c}_1}{\mathbf{a}_1} > \frac{c}{a}, \quad (18)$$

then we say that f satisfies cone conditions.

Example 9. This example stands behind the pictures from Figure 4. Consider $u = c = 1$ and $s = 0$. Assume that $f_{i_1 i_0} = (A_{ij}^1)_{i,j=1,2} = \text{diag}(\frac{1}{2}, 2)$, $f_{i_2 i_1} = (A_{ij}^2)_{i,j=1,2} = \text{diag}(2, 1)$,

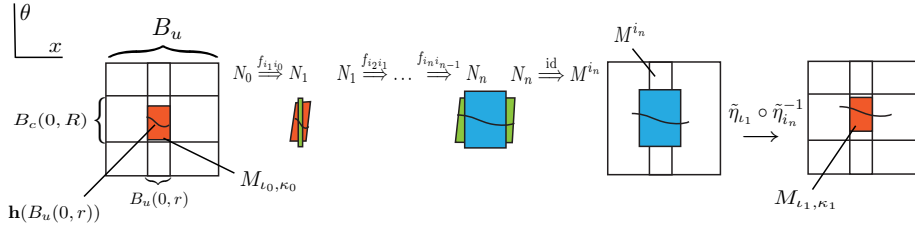


Figure 5. The sequence of covering relations from Definition 8, together with the sets M_{i_0, κ_0} and M_{i_1, κ_1} , which are the first step of the inductive construction from the proof of Theorem 10.

$f_{i_2 i_3} = (A_{ij}^3)_{i,j=1,2} = \text{diag}(5, 2)$. Let $\gamma_0 = (1, -1)$ and $\gamma_1 = (\frac{1}{4}, -\frac{3}{8})$. We take ch-sets with cones $(N_l((0, 0), r_u^l, r_c^l), \gamma_l)$, for $l = 0, 1, 2, 3$ with

$$\begin{aligned} r_u^0 &= r_c^0 = r, \\ r_u^l &= r_u^{l-1} A_{11}^l - \varepsilon, \\ r_c^l &= r_c^{l-1} A_{22}^l + \varepsilon, \end{aligned}$$

$\gamma_0 = \gamma_0$, $\gamma_1 = (4\delta, -\frac{1}{4}\delta^{-1})$, $\gamma_2 = (16\delta^2, -\frac{1}{4}\delta^{-2})$, $\gamma_3 = (\frac{1}{25}\delta^3, -\frac{1}{16}\delta^{-3})$, with $\delta = 1 + \varepsilon$. For sufficiently small r and ε we will have (16) and (17). For sufficiently small ε we also have (18). Assume now that $\tilde{\eta}_l \circ \tilde{\eta}_{i_3}^{-1} = \text{diag}(1, 1 + \frac{1}{4})$. This $\tilde{\eta}_l \circ \tilde{\eta}_{i_3}^{-1}$ is taken just as a hypothetical example, in order to show that even when a switch to new coordinates involves an expansion in the central coordinate the Assumption 7 can easily be satisfied. We have

$$\begin{aligned} Q_{\gamma_0}(\tilde{\eta}_l \circ \tilde{\eta}_{i_3}^{-1}(x, y)) &= x^2 - \frac{5}{4}\theta^2 \\ &= 4 \left(\frac{1}{4}x^2 - \frac{5}{16}\theta^2 \right) \\ &\geq 4 \left(\frac{1}{4}x^2 - \frac{3}{8}\theta^2 \right) \\ &= 4Q_{\gamma_1}((x, y)) \end{aligned}$$

which means that (14) holds for $\mathbf{m} < 4$.

We now introduce a notation $U \subset D_\phi$ for a set

$$U := B_u(0, r) \times B_s(0, r) \times \Lambda. \quad (19)$$

The set U will be the region in which we will construct an invariant manifold of points, which stay within the set D_ϕ for forward iterations of the map f_ϕ .

3.3. Existence of a normally hyperbolic manifold - Main result

In this section we use the assumptions from Section 3.2 to obtain the existence of a normally hyperbolic invariant manifold inside the set U defined in (19). We start with a construction of the center-stable manifold. This is given in Theorem 10. The existence of an center-unstable manifold follows from mirror arguments for the inverse map. The

normally hyperbolic manifold is obtained by intersecting the center-stable and center-unstable manifolds. This is done in Theorem 12.

Theorem 10. *If f satisfies cone conditions then there exists a continuous injective function $V : B_s(0, r) \times \Lambda \rightarrow U$ such that*

- (i) $\pi_y V(y, \lambda) = y$, $\pi_\lambda V(y, \lambda) = \lambda$,
- (ii) for any $(y, \lambda) \in B_s(0, r) \times \Lambda$ and any $n \in \mathbb{N}$

$$f_\phi^n(V(y, \lambda)) \in D_\phi,$$

- (iii) for any $q \in U$ such that $f_\phi^n(q) \in D_\phi$ for all $n \in \mathbb{N}$, there exists a $(y, \lambda) \in B_s(0, r) \times \Lambda$ such that $q = V(y, \lambda)$,

- (iv) if $\lambda^*, \lambda^{**} \in \eta_i^{-1}(B_c(\eta_i(\boldsymbol{\lambda}_k), \rho))$ for some $(i, k) \in J$ then for any $y^*, y^{**} \in \overline{B}_s(0, r)$ such that $(\lambda^*, y^*) \neq (\lambda^{**}, y^{**})$

$$Q_{\gamma_0}(\tilde{\eta}_i \circ V(y^*, \lambda^*) - \tilde{\eta}_i \circ V(y^{**}, \lambda^{**})) < 0. \quad (20)$$

Proof. We take any $y_0 \in B_s(0, r)$, $\lambda_0 \in \Lambda$ and $(\iota_0, \kappa_0) \in J$ such that $\lambda_0 \in \eta_{\iota_0}^{-1}(B_c(\boldsymbol{\lambda}_{\kappa_0}, \rho))$ and define a horizontal disc \mathbf{h}_0 in M_{ι_0, κ_0} as

$$\mathbf{h}_0(x) := (x, y_0, \eta_{\iota_0}(\lambda_0)).$$

Since f satisfies cone conditions, using assumption (16), applying inductively Lemma 5 gives us the existence of indexes $i_1, \dots, i_{n_1} \in I$ and of a horizontal disc \mathbf{h}_1 in (M, γ_{n_1}) such that

$$\begin{aligned} \mathbf{h}_1(\overline{B}_u) &= \{\tilde{\eta}_{i_{n_1}} \circ f_\phi^{n_1} \circ \tilde{\eta}_{\iota_0}^{-1}(\mathbf{h}_0(x)) \in M : x \in B_u(0, r), \text{ and} \\ &\quad \tilde{\eta}_{i_l} \circ f_\phi^l \circ \tilde{\eta}_{\iota_0}^{-1}(\mathbf{h}_0(x)) \in N_l \text{ for } l = 1, \dots, n_1\}. \end{aligned}$$

By (18), for $x^* \neq x^{**}$

$$Q_{\gamma_1}(\mathbf{h}_1(x^*) - \mathbf{h}_1(x^{**})) > Q_{\gamma_{n_1}}(\mathbf{h}_1(x^*) - \mathbf{h}_1(x^{**})) > 0,$$

which means that \mathbf{h}_1 is a horizontal disc in (M, γ_1) . From (14) and (15) we know that there exists $(\iota_1, \kappa_1) \in J$ such that $\mathbf{h}' := \tilde{\eta}_{\iota_1} \circ \tilde{\eta}_{i_{n_1}}^{-1} \circ \mathbf{h}_1$ is a horizontal disc in $(M_{\iota_1, \kappa_1}, \gamma_0)$. Let $\mathbf{f}_1 := \tilde{\eta}_{\iota_1} \circ f_\phi^{n_1} \circ \tilde{\eta}_{\iota_0}^{-1}$. For x for which $\tilde{\eta}_{i_{n_1}} \circ f_\phi^{n_1} \circ \tilde{\eta}_{\iota_0}^{-1}(\mathbf{h}_0(x)) \in \mathbf{h}_1(\overline{B}_u)$ we have:

$$\begin{aligned} \mathbf{f}_1(\mathbf{h}_0(x)) &= \tilde{\eta}_{\iota_1} \circ \tilde{\eta}_{i_{n_1}}^{-1} \circ \tilde{\eta}_{i_{n_1}} \circ f_\phi^{n_1} \circ \tilde{\eta}_{\iota_0}^{-1}(\mathbf{h}_0(x)) \\ &\subset \tilde{\eta}_{\iota_1} \circ \tilde{\eta}_{i_{n_1}}^{-1}(\mathbf{h}_1(\overline{B}_u)) \\ &= \mathbf{h}'(\overline{B}_u). \end{aligned}$$

This by (17) and (14) means that for any $x^* \neq x^{**}$ such that $\mathbf{h}_0(x^*), \mathbf{h}_0(x^{**}) \in \text{dom}(\mathbf{f}_1)$

$$Q_{\gamma_0}(\mathbf{f}_1(\mathbf{h}_0(x^*)) - \mathbf{f}_1(\mathbf{h}_0(x^{**}))) > \mathbf{m}Q_{\gamma_0}(\mathbf{h}_0(x^*) - \mathbf{h}_0(x^{**})) > 0. \quad (21)$$

Repeating the above procedure inductively (starting the second step with the horizontal disc \mathbf{h}' and local coordinates given by $\tilde{\eta}_{\iota_1}$) we obtain a sequence of points $x_s \in B_u(0, r)$ and indexes (ι_s, κ_s) for $s \in \mathbb{N}$ such that for

$$\mathbf{f}_s := \tilde{\eta}_{\iota_s} \circ f_\phi^{n_s + \dots + n_1} \circ \tilde{\eta}_{\iota_0}^{-1}$$

we have

$$\mathbf{f}_w(\mathbf{h}_0(x_s)) \in M_{l_w, \kappa_w} \quad \text{for } w \leq s.$$

Since $\overline{B}_u(0, r)$ is compact, there exists an $x_0 = x_0(y_0, \lambda_0) \in B_u(0, r)$ such that $\tilde{\eta}_{l_s}^{-1} \circ \mathbf{f}_s(\mathbf{h}_0(x_0)) \in U$ for all $s \in \mathbb{N}$.

For any two points x_0^*, x_0^{**} such that $\tilde{\eta}_{l_s}^{-1} \circ \mathbf{f}_s(\mathbf{h}_0(x_0^*)), \tilde{\eta}_{l_s}^{-1} \circ \mathbf{f}_s(\mathbf{h}_0(x_0^{**})) \in U$ for all $s \in \mathbb{N}$, if $x_0^* \neq x_0^{**}$ then by (21) we have

$$\begin{aligned} Q_{\gamma_0}(\mathbf{f}_s(\mathbf{h}_0(x_0^*)) - \mathbf{f}_s(\mathbf{h}_0(x_0^{**}))) &> \mathbf{m}Q_{\gamma_0}(\mathbf{f}_{s-1}(\mathbf{h}_0(x_0^*)) - \mathbf{f}_{s-1}(\mathbf{h}_0(x_0^{**}))) \\ &> \dots \\ &> \mathbf{m}^s Q_{\gamma_0}(\mathbf{h}_0(x_0^*) - \mathbf{h}_0(x_0^{**})) \\ &> 0. \end{aligned} \tag{22}$$

Since $\mathbf{m} > 1$, (22) implies in particular that if $x_0^* \neq x_0^{**}$, then

$$\|\pi_x(\mathbf{f}_s(\mathbf{h}_0(x_0^*)) - \mathbf{f}_s(\mathbf{h}_0(x_0^{**})))\| \rightarrow \infty \quad \text{as } s \rightarrow \infty.$$

Since $\mathbf{f}_s(\mathbf{h}_0(x_0^*)), \mathbf{f}_s(\mathbf{h}_0(x_0^{**}))$ are in M_{l_s, κ_s} , which is a subset of \mathbf{B} , which is bounded, we see that we must have $x_0^* = x_0^{**}$. This means that there is only a single point $x_0 = x_0(y_0, \lambda_0) \in B_u(0, r)$ such that $\tilde{\eta}_{l_s}^{-1} \circ \mathbf{f}_s(\mathbf{h}_0(x_0)) \in U$ for all $s \in \mathbb{N}$. We can thus define

$$V(y_0, \lambda_0) := \tilde{\eta}_{l_0}^{-1}(x_0(y_0, \lambda_0), y_0, \lambda_0).$$

We now need to show (20). Suppose that $V(y^*, \lambda^*), V(y^{**}, \lambda^{**}) \in M_{i, k}$ and $Q_{\gamma_0}(\tilde{\eta}_i \circ V(y^*, \lambda^*) - \tilde{\eta}_i \circ V(y^{**}, \lambda^{**})) \geq 0$. Applying estimates analogous to (22) we obtain a contradiction.

Continuity of V will follow from the fact that

$$Q_{\gamma_0}(\tilde{\eta}_{l_0} \circ V(y^*, \lambda^*) - \tilde{\eta}_{l_0} \circ V(y^{**}, \lambda^{**})) < 0. \tag{23}$$

Since $\gamma_0 = (\mathbf{a}_0, \mathbf{b}_0, \mathbf{c}_0)$ with $\mathbf{a}_0 > 0$ and $\mathbf{b}_0, \mathbf{c}_0 < 0$ (23) gives

$$\begin{aligned} 0 &> Q_{\gamma_0}(\tilde{\eta}_{l_0} \circ V(y^*, \lambda^*) - \tilde{\eta}_{l_0} \circ V(y^{**}, \lambda^{**})) \\ &= \mathbf{a}_0 \|\pi_x V(y^*, \lambda^*) - \pi_x V(y^{**}, \lambda^{**})\|^2 + \mathbf{b}_0 \|y^* - y^{**}\|^2 \\ &\quad + \mathbf{c}_0 \|\eta_{l_0}(\lambda^*) - \eta_{l_0}(\lambda^{**})\|^2, \end{aligned}$$

and therefore

$$\begin{aligned} &\mathbf{a}_0 \|\pi_x V(y^*, \lambda^*) - \pi_x V(y^{**}, \lambda^{**})\|^2 \\ &< \min(-\mathbf{b}_0, -\mathbf{c}_0) \|(y^*, \eta_{l_0}(\lambda^*)) - (y^{**}, \eta_{l_0}(\lambda^{**}))\|^2. \end{aligned}$$

□

Now we move to proving the existence of the normally hyperbolic invariant manifold. First we need a definition.

Definition 11. *We say that f satisfies backward cone conditions if f^{-1} satisfies cone conditions, with reversed roles of x and y coordinates.*

We assume that Assumption 7 holds for f with $\gamma_0 = \gamma_0^{\text{forw}}$. We assume also that for f^{-1} Assumption 7 holds with $\gamma_0 = \gamma_0^{\text{back}}$ (with reversed roles of the x and y coordinates).

Theorem 12. (Main Theorem) *Assume that f satisfies cone conditions for $\gamma_0^{\text{forw}} = (\mathbf{a}_0^f, \mathbf{b}_0^f, \mathbf{c}_0^f)$ and backward cone conditions with $\gamma_0^{\text{back}} = (\mathbf{a}_0^b, \mathbf{b}_0^b, \mathbf{c}_0^b)$. If*

$$|\mathbf{a}_0^f| > |\mathbf{a}_0^b| \quad \text{and} \quad |\mathbf{b}_0^f| < |\mathbf{b}_0^b| \quad (24)$$

then there exist continuous injective functions $W^s : B_s(0, r) \times \Lambda \rightarrow U$, $W^u : B_u(0, r) \times \Lambda \rightarrow U$ and $\chi : \Lambda \rightarrow U$, such that

$$\pi_{y,\lambda} W^s(y, \lambda) = (y, \lambda), \quad \pi_{x,\lambda} W^u(y, \lambda) = (x, \lambda), \quad \pi_\lambda \chi(\lambda) = \lambda, \quad (25)$$

and $\Lambda_\phi := \chi(\Lambda)$ is an invariant manifold for f_ϕ , with stable manifold $W^s(B_s(0, r) \times \Lambda)$ and unstable manifold $W^u(B_u(0, r) \times \Lambda)$.

Proof. Since f satisfies cone conditions, applying Theorem 10 we obtain $W^s(y, \lambda)$ as V . Since f satisfies backward cone conditions, once again from Theorem 10 for f^{-1} we also obtain $W^u(x, \lambda)$ as function V . From point (i) in Theorem 10 it follows that (25) holds for W^s and W^u .

We show that for any $\lambda \in \Lambda$ the sets $W^s(B_s(0, r), \lambda)$ and $W^u(B_u(0, r), \lambda)$ intersect. Let us define $F : B_u(0, r) \times B_s(0, r) \rightarrow B_u(0, r) \times B_s(0, r)$ as

$$F(x, y) := (\pi_x W^s(y, \lambda), \pi_y W^u(x, \lambda)).$$

Since F is continuous, from the Brouwer fixed point theorem follows that there exists an (x_0, y_0) such that $F(x_0, y_0) = (x_0, y_0)$. By (25) this means that

$$W^s(y_0, \lambda) = (\pi_x W^s(y_0, \lambda), y_0, \lambda) = (x_0, \pi_y W^u(x_0, \lambda), \lambda) = W^u(x_0, \lambda). \quad (26)$$

Now we show that for any given $\lambda \in \Lambda$ there exists only a single (x_0, y_0) satisfying (26). Suppose that for some $\lambda \in \Lambda$ there exist $(x^*, y^*), (x^{**}, y^{**}) \in B_u(0, r) \times B_s(0, r)$, $(x^*, y^*) \neq (x^{**}, y^{**})$ such that

$$W^s(y^*, \lambda) = W^u(x^*, \lambda) \quad \text{and} \quad W^s(y^{**}, \lambda) = W^u(x^{**}, \lambda).$$

From (25) we have $W^s(y_m, \lambda) = W^u(x_m, \lambda) = (x_m, y_m, \lambda)$ for $m = 1, 2$. From point (iv) in Theorem 10 follows that

$$\begin{aligned} Q_{\gamma_0^{\text{forw}}}(\tilde{\eta}_i \circ W^s(y^*, \lambda) - \tilde{\eta}_i \circ W^s(y^{**}, \lambda)) &= \\ Q_{\gamma_0^{\text{forw}}}((x^*, y^*, \eta_i(\lambda)) - (x^{**}, y^{**}, \eta_i(\lambda))) &< 0, \end{aligned}$$

$$\begin{aligned} Q_{\gamma_0^{\text{back}}}(\tilde{\eta}_i \circ W^u(x^*, \lambda) - \tilde{\eta}_i \circ W^u(x^{**}, \lambda)) &= \\ Q_{\gamma_0^{\text{back}}}((x^*, y^*, \eta_i(\lambda)) - (x^{**}, y^{**}, \eta_i(\lambda))) &< 0. \end{aligned}$$

which implies that

$$a_0^f \|x^* - x^{**}\|^2 + b_0^f \|y^* - y^{**}\|^2 < 0, \quad (27)$$

$$a_0^b \|x^* - x^{**}\|^2 + b_0^b \|y^* - y^{**}\|^2 < 0. \quad (28)$$

From (24) and (28) (keeping in mind that $a_0^f > 0$, $b_0^f < 0$ and that $a_0^b < 0$, $b_0^b > 0$ due to the reversion of the roles of x and y for the inverse map) it follows that

$$a_0^f \|x^* - x^{**}\|^2 > -a_0^b \|x^* - x^{**}\|^2 > b_0^b \|y^* - y^{**}\|^2 > -b_0^f \|y^* - y^{**}\|^2,$$

which contradicts (27).

We now define $\chi(\lambda) := (x_0, y_0, \lambda)$ for x_0, y_0 such that $W^s(y_0, \lambda) = W^u(x_0, \lambda)$. By the above arguments we know that χ is a properly defined function. We need to show that this function is continuous. Let us take any $\lambda^*, \lambda^{**} \in \eta_i^{-1}(B_c(\eta_i(\lambda_k), \rho))$ for some $(i, k) \in J$. From point (iv) in Theorem 10 it follows that

$$\begin{aligned} Q_{\gamma_0^{\text{forw}}}(\tilde{\eta}_i \circ \chi(\lambda^*) - \tilde{\eta}_i \circ \chi(\lambda^{**})) &< 0, \\ Q_{\gamma_0^{\text{back}}}(\tilde{\eta}_i \circ \chi(\lambda^*) - \tilde{\eta}_i \circ \chi(\lambda^{**})) &< 0. \end{aligned} \tag{29}$$

Let us adopt the notations $\tilde{\eta}_i \circ \chi(\lambda^*) = (x^*, y^*, \theta^*)$ and $\tilde{\eta}_i \circ \chi(\lambda^{**}) = (x^{**}, y^{**}, \theta^{**})$. Note that from the construction of χ follows that $\eta_i(\lambda^*) = \theta^*$ and $\eta_i(\lambda^{**}) = \theta^{**}$. From (29) it follows that

$$\begin{aligned} (a_0^f + a_0^b) \|x^* - x^{**}\|^2 + (b_0^f + b_0^b) \|y^* - y^{**}\|^2 \\ < - (c_0^f + c_0^b) \|\theta^* - \theta^{**}\|^2 \\ = - (c_0^f + c_0^b) \|\eta_i(\lambda^*) - \eta_i(\lambda^{**})\|^2 \end{aligned} \tag{30}$$

From (24) it follows that $a_0^f + a_0^b = |a_0^f| - |a_0^b| > 0$ and $b_0^f + b_0^b = -|b_0^f| + |b_0^b| > 0$. By the fact that η_i is continuous and the fact that $c_0^f < 0$ and $c_0^b < 0$, from (30) follows the continuity of χ .

We will now show that for any $p \in W^s(B_s(0, r) \times \Lambda)$, $f_\phi^n(p)$ converges to $\chi(\Lambda)$ as n goes to infinity. Let us consider the limit set of the point p

$$\omega(f_\phi, p) = \{q \mid \lim_{k \rightarrow \infty} f_\phi^{n_k}(p) = q \text{ for some } n_k \rightarrow \infty\}.$$

If we can show that $\omega(f_\phi, p)$ is contained in $W^u \cap W^s = \chi(\Lambda)$, then this will conclude the proof of Theorem 12. We take any $q = \lim_{k \rightarrow \infty} f_\phi^{n_k}(p)$ from $\omega(f_\phi, p)$. By continuity of W^s we know that $q \in W^s$. Suppose now that $q \notin W^u$. This would mean that there exists an $n > 0$ for which $f_\phi^{-n}(q) \notin B_u(0, r) \times B_s(0, r) \times \Lambda$. Since

$$\lim_{k \rightarrow \infty} f_\phi^{n_k - n}(p) = f_\phi^{-n}(q),$$

we have that $f_\phi^{-n}(q) \in \omega(f_\phi, p)$, but this contradicts the fact that $\omega(f_\phi, p) \subset B_u(0, r) \times B_s(0, r) \times \Lambda$.

Showing that all backward iterations of points in $W^u(B_u(0, r) \times \Lambda)$ converge to $\chi(\Lambda)$ is analogous. \square

Remark 13. Let us note that during the course of the proof of Theorem 12 we have established more than just continuity of W^u , W^s and χ . From our construction we

know that for $i \in I$

$$\begin{aligned}\tilde{\eta}_i \circ W^u(x, \eta_i^{-1}(\theta)) &= (x, w_i^u(x, \theta), \theta), \\ \tilde{\eta}_i \circ W^s(y, \eta_i^{-1}(\theta)) &= (w_i^s(y, \theta), y, \theta), \\ \tilde{\eta}_i \circ \chi(\eta_i^{-1}(\theta)) &= (\varkappa_i(\theta), \theta),\end{aligned}$$

for continuous $w_i^u : B_u(0, r) \times B_c \rightarrow B_s(0, r)$, $w_i^s : B_s(0, r) \times B_c \rightarrow B_u(0, r)$ and $\varkappa_i : B_c \rightarrow B_u(0, r) \times B_s(0, r)$. The inequality (20) from Theorem 10 can be used to obtain explicit Lipschitz bounds for functions w_i^u , w_i^s . Also estimates (30) can be used to obtain Lipschitz bounds for \varkappa_i . This means that we can get Lipschitz estimates for the invariant manifold $\chi(\Lambda)$ together with Lipschitz estimates for its stable and unstable manifold.

4. Verification of covering and cone conditions

In this section we show how covering relations and cone conditions can be verified with the use of local bounds on derivatives. The idea is to develop a simple automatised scheme which could be applied in computer assisted proofs. In our approach we set up our verification so that we do not need to compute images of large sets (which in case of rigorous numerics is always troublesome). The scheme is based on iterates of a number of single points, combined with estimates on derivatives around their neighbourhoods.

For any set $V \subset \mathbb{R}^n$ we define the interval enclosure of the derivative of f on V as

$$[df(V)] := \left\{ A \in \mathbb{R}^{n \times n} \mid A_{ij} \in \left[\inf_{q \in V} \frac{df_i}{dq_j}(q), \sup_{q \in V} \frac{df_i}{dq_j}(q) \right] \text{ for all } i, j = 1, \dots, n \right\}.$$

Let $U_{i_1}, U_{i_2} \subset \Lambda$ be such that $\text{dom} f_{i_2 i_1}$ is nonempty (here we use $\text{dom} f_{i_2 i_1}$ to denote the domain of $f_{i_2 i_1}$). Assume that for any $(c + u + s) \times (c + u + s)$ matrix

$$A \in [df_{i_2 i_1}(\text{dom} f_{i_2 i_1})] \tag{31}$$

we have the following bounds

$$\begin{aligned}\sup \{ \|A_{kl} v_l\| : \|v_l\| = 1 \} &\leq \overline{A}_{kl}, \\ \inf \{ \|A_{kl} v_l\| : \|v_l\| = 1 \} &\geq \underline{A}_{kl},\end{aligned} \tag{32}$$

with $k, l \in \{x, y, \theta\}$ and v_x, v_y, v_θ representing the variables x, y, θ respectively (note that $\overline{A}_{kl}, \underline{A}_{kl}$ depend on the choice of $i_2 i_1$). In this section we shall use the bounds (32), together with pointwise bounds on the function f , for verification of covering and cone conditions.

4.1. Verifying covering conditions

We define a 3×3 matrix $T_{i_2 i_1}$ as

$$T_{i_2 i_1} := (t_{kl})_{k, l \in \{x, y, \theta\}}$$

$$\begin{aligned}
t_{xx} &= \underline{A}_{xx}, & t_{xy} &= -\overline{A}_{xy}, & t_{x\theta} &= -\overline{A}_{x\theta}, \\
t_{yx} &= \overline{A}_{yx}, & t_{yy} &= \overline{A}_{yy}, & t_{y\theta} &= \overline{A}_{y\theta}, \\
t_{\theta x} &= \overline{A}_{\theta x}, & t_{\theta y} &= \overline{A}_{\theta y}, & t_{\theta\theta} &= \overline{A}_{\theta\theta}.
\end{aligned} \tag{33}$$

We will use notations $R = (r_u, r_s, r_c) \in \mathbb{R}^3$ and for $q = (x, y, \theta) \in \mathbb{R}^u \times \mathbb{R}^s \times \mathbb{R}^c$ and write

$$N(q, R) := N(q, r_u, r_s, r_c).$$

We give a lemma, which can be used in order to verify that $N_1 \xrightarrow{f_{i_2 i_1}} N_2$.

Lemma 14. *Let $\varepsilon > 0$ be a small number. Let $N_1 = N(q_1, R_1) \subset \text{dom} f_{i_2 i_1}$ be a ch-set. If for $R_2 = (r_u^2, r_s^2, r_c^2) := T_{i_2 i_1} R_1 + (-\varepsilon, \varepsilon, \varepsilon)$ we have $r_u^2, r_s^2, r_c^2 > 0$ and for $q_2 := f_{i_2 i_1}(q_1)$*

$$\|\pi_x q_2\| + r_u^2 \leq 1, \quad \|\pi_y q_2\| + r_s^2 \leq 1, \quad \|\pi_\theta q_2\| + r_c^2 \leq 1, \tag{34}$$

then for $N_2 := N(q_2, R_2)$ we have $N_1 \xrightarrow{f_{i_2 i_1}} N_2$.

Proof. Condition (1) holds by the choice of q_2 and N_2 . Let $q \in N_1^-$, then for

$$A := \int_0^1 Df_{i_2 i_1}(q_1 + t(q - q_1)) dt \in [df_{i_2 i_1}(\text{dom} f_{i_2 i_1})],$$

we have estimates

$$\begin{aligned}
\|\pi_x(f_{i_2 i_1}(q) - q_2)\| &= \|\pi_x(f_{i_2 i_1}(q) - f_{i_2 i_1}(q_1))\| \\
&= \left\| \pi_x \left(\int_0^1 Df_{i_2 i_1}(q_1 + t(q - q_1)) dt \cdot (q - q_1) \right) \right\| \\
&= \|\pi_x A(q - q_1)\| \\
&= \|A_{xx}\pi_x(q - q_1) + A_{xy}\pi_y(q - q_1) + A_{x\theta}\pi_\theta(q - q_1)\| \\
&\geq \underline{A}_{xx}r_u^1 - \overline{A}_{xy}r_s^1 - \overline{A}_{x\theta}r_c^1 \\
&> r_u^2,
\end{aligned}$$

hence (2) holds. Analogous computations for $q \in N_1$ give

$$\begin{aligned}
\|\pi_y(f_{i_2 i_1}(q) - q_2)\| &= \|\pi_y A(q - q_1)\| \leq \overline{A}_{yx}r_u^1 + \overline{A}_{yy}r_s^1 + \overline{A}_{y\theta}r_c^1 < r_s^2, \\
\|\pi_\theta(f_{i_2 i_1}(q) - q_2)\| &= \|\pi_\theta A(q - q_1)\| \leq \overline{A}_{\theta x}r_u^1 + \overline{A}_{\theta y}r_s^1 + \overline{A}_{\theta\theta}r_c^1 < r_c^2,
\end{aligned}$$

which proves (3). Conditions (34) ensure that $N_2 \subset \mathbf{B}$. \square

Example 15. We return to our Example 9. The ch-sets from the example follow from Lemma 8 as $N_l = N(0, R_l)$ where $R_0 = (r, r)$ and $R_{l+1} = T_{i_{l+1} i_l} R_l + (-\varepsilon, \varepsilon, \varepsilon)$ with $T_{i_{l+1} i_l} = \text{diag}(A_{11}^{l+1}, A_{22}^{l+1})$.

Remark 16. When the x coordinate is strongly expanding, for practical reasons it might be beneficial to set r_u^2 significantly smaller than $\pi_x T_{i_2 i_1} R_1$. In such case the covering $N_1 \xrightarrow{f_{i_2 i_1}} N_2$ will still take place, but N_2 will be a smaller set. This might give better bounds for next iterations of the map f and also keep the later constructed N_i within \mathbf{B} . Without reducing r_u , in the case when x is rapidly expanding, it might turn out that the sets N_i blow up quickly.

4.2. Verifying cone conditions

Now we shall present some lemmas, which will show how one can obtain condition (17), from bounds on derivatives (32). The aim is to present a simple mechanism in which successive γ_l are constructed.

Let $C = (c_{ij})_{i,j=\{x,y,\theta\}}$ be a 3×3 matrix with coefficients

$$\begin{aligned} c_{xx} &= \underline{A}_{xx}^2 - \sum_{k \neq x} \bar{A}_{xx} \bar{A}_{xk}, & c_{xy} &= \sum_{k \in \{x,y,\theta\}} \bar{A}_{yx} \bar{A}_{yk}, & c_{x\theta} &= \sum_{k \in \{x,y,\theta\}} \bar{A}_{\theta x} \bar{A}_{\theta k}, \\ c_{yx} &= \underline{A}_{xy}^2 - \sum_{k \neq y} \bar{A}_{xy} \bar{A}_{xk}, & c_{yy} &= \sum_{k \in \{x,y,\theta\}} \bar{A}_{yy} \bar{A}_{yk}, & c_{y\theta} &= \sum_{k \in \{x,y,\theta\}} \bar{A}_{\theta y} \bar{A}_{\theta k}, \\ c_{\theta x} &= \underline{A}_{x\theta}^2 - \sum_{k \neq \theta} \bar{A}_{x\theta} \bar{A}_{xk}, & c_{\theta y} &= \sum_{k \in \{x,y,\theta\}} \bar{A}_{y\theta} \bar{A}_{yk}, & c_{\theta\theta} &= \sum_{k \in \{x,y,\theta\}} \bar{A}_{\theta\theta} \bar{A}_{\theta k}, \end{aligned} \quad (35)$$

(note that C depends on the choice of i_2, i_1).

We start with a technical lemma

Lemma 17. *Let $\gamma = (a, b, c) \in \mathbb{R}^3$ and let $A : \mathbb{R}^{u+s+c} \rightarrow \mathbb{R}^{u+s+c}$ be a matrix for which the bounds (32) hold. If $a \geq 0, b \leq 0, c \leq 0$ then for any $p = (p_x, p_y, p_\theta) \in \mathbb{R}^c \times \mathbb{R}^u \times \mathbb{R}^s$*

$$Q_\gamma(Ap) \geq Q_{C\gamma}(p).$$

Proof. Using the estimate

$$\pm 2 \langle A_{kl} p_l, A_{kj} p_j \rangle \geq -\bar{A}_{kl} \bar{A}_{kj} (\|p_l\|^2 + \|p_j\|^2)$$

we obtain (below, for inequality $<$ between indexes we use alphabetic order $x < y < \theta$)

$$\begin{aligned} & Q_\gamma(Ap) \\ &= a \sum_{l,j \in \{x,y,\theta\}} \langle A_{xl} p_l, A_{xj} p_j \rangle + b \sum_{l,j \in \{x,y,\theta\}} \langle A_{yl} p_l, A_{yj} p_j \rangle + c \sum_{l,j \in \{x,y,\theta\}} \langle A_{\theta l} p_l, A_{\theta j} p_j \rangle \\ &= a \sum_{k \in \{x,y,\theta\}} \|A_{xk} p_k\|^2 + b \sum_{k \in \{x,y,\theta\}} \|A_{yk} p_k\|^2 + c \sum_{k \in \{x,y,\theta\}} \|A_{\theta k} p_k\|^2 \\ &\quad + 2 \sum_{l < j} a \langle A_{xl} p_l, A_{xj} p_j \rangle + 2 \sum_{l < j} b \langle A_{yl} p_l, A_{yj} p_j \rangle + 2 \sum_{l < j} c \langle A_{\theta l} p_l, A_{\theta j} p_j \rangle \\ &\geq \|p_x\|^2 (a \underline{A}_{xx}^2 + b \bar{A}_{yx}^2 + c \bar{A}_{\theta x}^2) + \|p_y\|^2 (a \underline{A}_{xy}^2 + b \bar{A}_{yy}^2 + c \bar{A}_{\theta y}^2) \\ &\quad + \|p_\theta\|^2 (a \underline{A}_{x\theta}^2 + b \bar{A}_{y\theta}^2 + c \bar{A}_{\theta\theta}^2) \\ &\quad - a \sum_{l < j} \bar{A}_{xl} \bar{A}_{xj} (\|p_l\|^2 + \|p_j\|^2) + b \sum_{l < j} \bar{A}_{yl} \bar{A}_{yj} (\|p_l\|^2 + \|p_j\|^2) \\ &\quad + c \sum_{l < j} \bar{A}_{\theta l} \bar{A}_{\theta j} (\|p_l\|^2 + \|p_j\|^2) \\ &= (C\gamma)_x \|p_x\|^2 + (C\gamma)_y \|p_y\|^2 + (C\gamma)_\theta \|p_\theta\|^2. \end{aligned}$$

□

Now we give a lemma which will be the main tool in the construction of γ_l from Definition 8.

Lemma 18. *Let $U_{i_1}, U_{i_2} \subset \Lambda$ and let N be a ch-set $N \subset \text{dom}(f_{i_2 i_1})$. Let $\varepsilon > 0$ be a small number. Let C be defined by (35) and $\varepsilon > 0$. Assume that C is invertible and define*

$$G_{i_2 i_1} = C^{-1}. \quad (36)$$

If for $\gamma' = (a, b, c) := G_{i_2 i_1} \gamma + (\varepsilon, \varepsilon, \varepsilon)$, we have $a > 0$, and $b, c < 0$ then for any $q_1, q_2 \in N$

$$Q_{\gamma'}(f_{i_2 i_1}(q_1) - f_{i_2 i_1}(q_2)) > Q_{\gamma}(q_1 - q_2).$$

Proof. For

$$A := \int_0^1 Df_{i_2 i_1}(q_2 + t(q_1 - q_2)) dt \in [df_{i_2 i_1}(\text{dom} f_{i_2 i_1})]$$

applying Lemma 17 gives

$$\begin{aligned} Q_{\gamma'}(f_{i_2 i_1}(q_1) - f_{i_2 i_1}(q_2)) &> Q_{G_{i_2 i_1} \gamma}(f_{i_2 i_1}(q_1) - f_{i_2 i_1}(q_2)) \\ &\geq Q_{CG_{i_2 i_1} \gamma}(q_1 - q_2) \\ &= Q_{\gamma}(q_1 - q_2). \end{aligned}$$

□

Example 19. We return to Example 9. The cones γ_l follow from Lemma 18 as $\gamma_0 = (1, -1)$ and $\gamma_{l+1} = (1 + \varepsilon, (1 + \varepsilon)^{-1}) \cdot G_{i_{l+1} i_l} \gamma_l$ with $G_{i_{l+1} i_l} = \text{diag} \left(\frac{1}{(A_{11}^{l+1})^2}, \frac{1}{(A_{22}^{l+1})^2} \right)$, where \cdot stands for the scalar product.

4.3. Setting up local maps

In this section we shall introduce conditions, which ensure that the assumptions from Section 3.2 hold. Below we give a Lemma which ensures (14) and (15) hold under conditions easier to check.

Let us note that in some cases conditions (14) and (15) will follow from easier arguments or directly from the setup of the problem. Such is the case in our example from Section 5.

Lemma 20. *Let $\mathbf{m} > 1$, $\Delta > 0$ and $\rho > \sqrt{\frac{\mathbf{a}_0}{-\mathbf{c}_0}} r + \Delta$. Assume that*

(i) for any $\iota \in I$ and any $\lambda \in U_\iota$ there exists a $\boldsymbol{\lambda}_\kappa$ such that $(\iota, \kappa) \in J$ and

$$\|\eta_\iota(\lambda) - \eta_\iota(\boldsymbol{\lambda}_\kappa)\| < \Delta, \quad (37)$$

(ii) for any $\theta \in B_c$ and any $i \in I$ there exists an $\iota \in I$ such that

$$\overline{B}_c \left(\theta, \sqrt{\frac{\mathbf{a}_1}{-\mathbf{c}_1}} r \right) \cap \overline{B}_c \subset \text{dom}(\eta_\iota \circ \eta_i^{-1}), \quad (38)$$

$$\eta_\iota \circ \eta_i^{-1}(\theta) \in B_c(0, R - \rho - \Delta), \quad (39)$$

(iii) For $i, \iota \in I$ for which (39)–(38) hold, and for $C_{\iota i}$ defined as in (35), constructed for $[d(\tilde{\eta}_\iota \circ \tilde{\eta}_i^{-1})(\text{dom}(\eta_\iota \circ \eta_i^{-1}))]$, we assume that $C_{\iota i}$ is invertible and also that for $\gamma = (a, b, c) = C_{\iota i}^{-1}\gamma_1$ we have

$$\mathbf{a}_0 > \mathbf{m}a, \quad \mathbf{b}_0 > \mathbf{m}b, \quad \mathbf{c}_0 > \mathbf{m}c. \quad (40)$$

Then for any horizontal disc \mathbf{h} in a ch-set with cones (M, γ_1) and for any $i \in I$ there exists $(\iota, \kappa) \in J$ such that $\mathbf{h}(\overline{B}_u(0, r)) \subset \text{dom}(\tilde{\eta}_\iota \circ \tilde{\eta}_i^{-1})$. Also for any q_1, q_2 in $\text{dom}(\tilde{\eta}_\iota \circ \tilde{\eta}_i^{-1})$ such that $Q_{\gamma_1}(q_1 - q_2) > 0$ we have (14). Furthermore condition (15) holds.

Proof. Let \mathbf{h} be a horizontal disc in a ch-set with cones (M, γ_1) . Take $\theta_0 = \pi_\theta(\mathbf{h}(0))$. For any $x \in \overline{B}_u(0, r)$ we have $Q_{\gamma_1}(\mathbf{h}(x) - \mathbf{h}(0)) \geq 0$, which implies that

$$\mathbf{a}_1 r^2 \geq \mathbf{a}_1 \|\pi_x(\mathbf{h}(x) - \mathbf{h}(0))\|^2 \geq -\mathbf{c}_1 \|\pi_\theta(\mathbf{h}(x)) - \theta_0\|^2,$$

hence $\pi_\theta(\mathbf{h}(\overline{B}_u(0, r))) \subset \overline{B}_c(\theta_0, \sqrt{\frac{\mathbf{a}_1}{-\mathbf{c}_1}}r) \cap \overline{B}_c$. Taking ι from assumption (ii) for $\theta = \theta_0$, condition (38) implies that $\mathbf{h}(\overline{B}_u(0, r)) \subset \text{dom}(\tilde{\eta}_\iota \circ \tilde{\eta}_i^{-1})$ and also

$$\|\eta_\iota \circ \eta_i^{-1}(\theta_0)\| < R - \rho - \Delta. \quad (41)$$

Take now any q_1, q_2 in $\text{dom}(\tilde{\eta}_\iota \circ \tilde{\eta}_i^{-1})$ such that $Q_{\gamma_1}(q_1 - q_2) > 0$. Applying (40) and Lemma 18 gives

$$\begin{aligned} Q_{\gamma_0}(\tilde{\eta}_\iota \circ \tilde{\eta}_i^{-1}(q_1) - \tilde{\eta}_\iota \circ \tilde{\eta}_i^{-1}(q_2)) &> \mathbf{m}Q_\gamma(\tilde{\eta}_\iota \circ \tilde{\eta}_i^{-1}(q_1) - \tilde{\eta}_\iota \circ \tilde{\eta}_i^{-1}(q_2)) \\ &\geq \mathbf{m}Q_{C_{\iota i}C_{\iota i}^{-1}\gamma_1}(q_1 - q_2) \\ &= \mathbf{m}Q_{\gamma_1}(q_1 - q_2) \\ &> 0, \end{aligned} \quad (42)$$

which proves (14). Applying the bound in (42) for $q_1 = \mathbf{h}(x_1)$, $q_2 = \mathbf{h}(x_2)$ gives

$$Q_{\gamma_0}(\mathbf{h}'(x_1) - \mathbf{h}'(x_2)) \geq 0, \quad (43)$$

which means that to prove (15) it is sufficient to show that $\mathbf{h}'(\overline{B}_u(0, r)) \subset M_{\iota, \kappa}$ for some κ . Let $\lambda = \eta_i^{-1}(\theta_0)$. We now take κ from assumption (i). For any $x \in \overline{B}_u(0, r)$, by (43) we have

$$\begin{aligned} \mathbf{a}_0 r^2 &\geq \mathbf{a}_0 \|\pi_x(\mathbf{h}'(x) - \mathbf{h}'(0))\|^2 \\ &\geq -\mathbf{c}_0 \|\pi_\theta(\mathbf{h}'(x) - \mathbf{h}'(0))\|^2 \\ &= -\mathbf{c}_0 \|\pi_\theta(\mathbf{h}'(x)) - \eta_\iota(\lambda)\|^2. \end{aligned}$$

This means that

$$\pi_\theta(\mathbf{h}'(\overline{B}_u(0, r))) \subset \overline{B}_c(\eta_\iota(\lambda), r\sqrt{\frac{\mathbf{a}_0}{-\mathbf{c}_0}})$$

and hence

$$\begin{aligned} \|\pi_\theta(\mathbf{h}'(x)) - \eta_\iota(\boldsymbol{\lambda}_\kappa)\| &\leq \|\pi_\theta(\mathbf{h}'(x)) - \eta_\iota(\lambda)\| + \|\eta_\iota(\lambda) - \eta_\iota(\boldsymbol{\lambda}_\kappa)\| \\ &< r\sqrt{\frac{\mathbf{a}_0}{-\mathbf{c}_0}} + \Delta \\ &< \rho, \end{aligned}$$

which gives $\mathbf{h}'(\overline{B}_u(0, r)) \subset M_{\iota, \kappa}$. The last property that needs to be verified is that $M_{\iota, \kappa} \subset \mathbf{B}$. From our construction $\pi_\theta M_{\iota, \kappa} = \overline{B}_c(\eta_\iota(\boldsymbol{\lambda}_\kappa), \rho)$. For $\theta \in \overline{B}_c(\eta_\iota(\boldsymbol{\lambda}_\kappa), \rho)$, using (37) and (41)

$$\begin{aligned} \|\theta\| &\leq \|\theta - \eta_\iota(\boldsymbol{\lambda}_\kappa)\| + \|\eta_\iota(\boldsymbol{\lambda}_\kappa) - \eta_\iota(\lambda)\| + \|\eta_\iota(\lambda)\| \\ &= \|\theta - \eta_\iota(\boldsymbol{\lambda}_\kappa)\| + \|\eta_\iota(\boldsymbol{\lambda}_\kappa) - \eta_\iota(\lambda)\| + \|\eta_\iota \circ \eta_i^{-1}(\theta_0)\| \\ &< \rho + \Delta + (R - \rho - \Delta), \end{aligned}$$

hence $\pi_\theta M_{\iota, \kappa} \subset B_c$. □

4.4. Normally hyperbolic manifolds from bounds on derivatives

In Section 4.1 we have shown how covering relations from the chain (16) can be constructed using point-wise bounds together with bounds on derivatives of local maps. In Section 4.2 we have shown how the cones can be set up, using bounds on derivatives of local maps, so that the condition (17) holds. Here we shall combine these results together in Theorem 12.

We shall use the notations $T_{i_2 i_1}$ and $G_{i_2 i_1}$ introduced in Sections 4.1, 4.2 through equations (33), (35) and (36). We will also assume that the assumptions from Section 3.2 hold. Here we introduce a definition which contains conditions which can be verified using computer assistance. We will later show that the conditions imply cone conditions.

Definition 21. *Assume that for any $(\iota_0, \kappa_0) \in J$ there exists an $n \in \mathbb{N}$, a sequence $\iota_0 = i_0, i_1, \dots, i_n = \iota_1$ and κ_1 such that $(\iota_1, \kappa_1) \in J$ and for*

$$\begin{aligned} q^m &= (x^m, y^m, \theta^m) := f_{i_m i_{m-1}} \circ \dots \circ f_{i_1 i_0}(0, 0, \eta_{i_0}(\boldsymbol{\lambda}_{\kappa_0})), \\ R^m &= (r_u^m, r_s^m, r_c^m) := T_{i_m i_{m-1}} \circ \dots \circ T_{i_1 i_0}(r, r, \rho), \\ \gamma^m &:= (a^m, b^m, c^m) := G_{i_m i_{m-1}} \circ \dots \circ G_{i_1 i_0} \gamma_0 \end{aligned}$$

with $m \leq n$ we have

$$\begin{aligned} r_u^m + \|x^m\| &< 1, & r_s^m + \|y^m\| &< 1, & r_c^m + \|\theta^m\| &< 1, \\ r_u^n &> r + \|x^n\|, & r_s^n + \|y^n\| &< r, \end{aligned} \tag{44}$$

and

$$\begin{aligned} a^m &> 0, & 0 &> b^m, & 0 &> c^m, \\ a^n &> \mathbf{a}_1, & b^n &> \mathbf{b}_1, & c^n &> \mathbf{c}_1. \end{aligned}$$

Then we say that f satisfies forward bounds.

Remark 22. To verify that f satisfies forward bounds one needs to compute q^m , R^m and γ^m . Let us note that in the case of q^m it is enough to obtain bounds on a finite number of successive iterates of a single point. We therefore do not need to obtain bounds on images of large sets, which in practice would accumulate large errors. The R^m and γ^m are constructed using local bounds on derivatives and are easily computable with computer assistance. Let us also note that to verify forward bounds we do not need to compute the composition function f^n or its derivative (though there are ways of overcoming this, it could likely cause big difficulties for high n due to complexity of such computations and also due to the fact that errors would accumulate quickly).

Lemma 23. *If f satisfies forward bounds in the sense of Definition 21, then f satisfies cone conditions.*

Proof. We take any $(\iota_0, \kappa_0) \in J$, a sequence $\iota_0 = i_0, i_1, \dots, i_n = \iota_1$ and an index κ_1 such that $(\iota_1, \kappa_1) \in J$ from Definition 21. We define $R^0 = R_\varepsilon^0 := (r, r, \rho)$ and

$$\begin{aligned} R_\varepsilon^m &:= T_{i_m i_{m-1}} R_\varepsilon^{m-1} + (-\varepsilon, \varepsilon, \varepsilon), \\ N_m &:= N(q^m, R_\varepsilon^m). \end{aligned}$$

By (44), taking ε sufficiently small, we will ensure that $N_m \subset \mathbf{B}$. By Lemma 14 we obtain $N_{m-1} \xrightarrow{f_{i_m i_{m-1}}} N_m$ for $m = 1, \dots, n$ and $N_n \xrightarrow{\text{id}} M$.

Now we define $\gamma^0 = \gamma_\varepsilon^0 := \gamma_0$ and

$$\gamma_\varepsilon^m := G_{i_m i_{m-1}} \gamma_\varepsilon^{m-1} + (\varepsilon, \varepsilon, \varepsilon).$$

Taking $\varepsilon > 0$ small enough and applying Lemma 18 we obtain (17). \square

From now on let us assume that f satisfies forward bounds with $\gamma_0 = \gamma_0^{\text{forw}}$.

Definition 24. *Let $\gamma_0^{\text{back}} = (\mathbf{a}_0^{\text{b}}, \mathbf{b}_0^{\text{b}}, \mathbf{c}_0^{\text{b}}) \in \mathbb{R}^3$ be such that $\mathbf{a}_0^{\text{b}}, \mathbf{c}_0^{\text{b}} < 0$ and $\mathbf{b}_0^{\text{b}} > 0$. We say that f satisfies backward bounds if f^{-1} satisfies forward bounds, with reversed roles of the x and y coordinates.*

Theorem 25. *Assume that f satisfies forward bounds for $\gamma_0^{\text{forw}} = (\mathbf{a}_0^{\text{f}}, \mathbf{b}_0^{\text{f}}, \mathbf{c}_0^{\text{f}})$ and backward bounds for $\gamma_0^{\text{back}} = (\mathbf{a}_0^{\text{b}}, \mathbf{b}_0^{\text{b}}, \mathbf{c}_0^{\text{b}})$. If in addition inequality (24) holds then there exists a normally hyperbolic invariant manifold in \mathcal{U} , together with its stable and unstable manifolds W^s, W^u .*

Proof. This follows directly from Lemma 23 and Theorem 12. \square

5. Example of applications

Consider a driven logistic map

$$\begin{aligned} T : S^1 \times \mathbb{R} &\rightarrow S^1 \times \mathbb{R}, \\ T(\theta, x) &= (\theta + \alpha, 1 - a(\theta)x^2), \quad a(\theta) = a_0 + \varepsilon \sin(2\pi\theta) \end{aligned} \tag{45}$$

which differs from the well-known logistic map in the fact that the parameter a has been replaced by $a_0 + \varepsilon \sin(2\pi\theta)$ and θ has a quasiperiodic dynamics. Concretely we

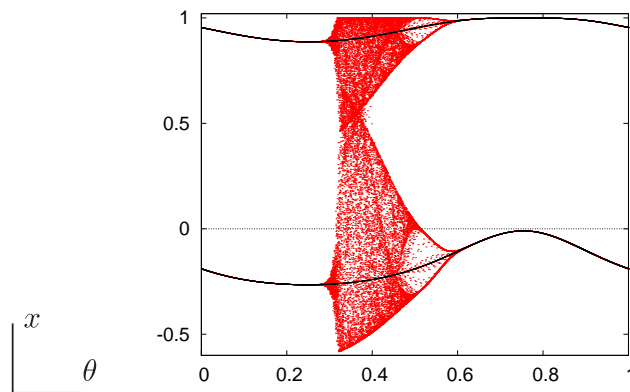


Figure 6. Misleading numerical plot of the attractor for T , obtained using **double precision** (consisting of points), and the true invariant curves computed with 128bit accuracy.

consider the parameter values $a_0 = 1.31$, $\varepsilon = 0.3$ and $\alpha = \frac{g}{200}$, where g is the golden mean $g = \frac{\sqrt{5}-1}{2}$. Hence the dynamics on the base of the skew-product is slow. Numerical simulations in **double precision** (say, with mantissa of 52 binary digits) suggest that the map possesses a chaotic global attractor (see Figure 6). We will prove that this guess is not correct. When the same simulations are done with multiple precision, one can guess that the attractor consists of two invariant curves (see Figure 6). We will use the method introduced in the previous sections to prove that T possesses a contracting invariant manifold and, in particular, that the plot obtained using **double precision** (Figure 6) does not show the true dynamics. The same example was considered for other values of α and in a non-rigorous way in [2] to illustrate that one has to be careful with the arithmetics in simulations. We can refer to [11] for additional examples in a similar context.

5.1. Explaining the observed behaviour

To explain the reasons of the observed behaviour it is worth to mention that in the example the parameter a of the logistic map ranges in $[a_0 - \varepsilon, a_0 + \varepsilon] = [1.01, 1.61]$. For that range the attractor starts as a recently created (at $a = 1$) period-2 sink, followed by the full period-doubling cascade. Then one finds from several-pieces strange attractors to a single piece, interrupted by some periodic sinks and its corresponding cascades. When a moves with θ one can question which is the “averaged” behaviour. In particular the period-2 orbit is only attracting until $a = 5/4$.

To this end we can consider what happens for “frozen” values of a , denoting as T_a the corresponding logistic map. The orbit of period two, $x_1(a), x_2(a)$ is given by the solutions of $x^2 - x/a + (1-a)/a^2$. In particular

$$x_1(a) = (1 - \sqrt{4a - 3})/(2a). \quad (46)$$

The differential of T_a^2 on it is $4(1-a)$. To average with respect to θ along the range,

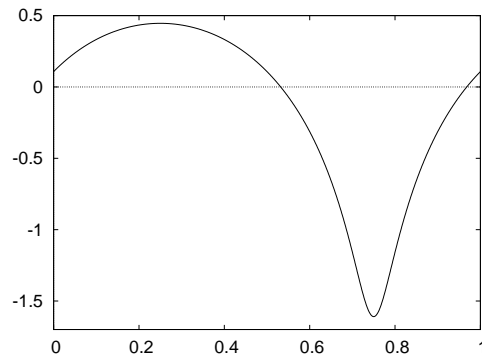


Figure 7. The integrand $h(\theta)$ in (47) for the parameter values: $a_0 = 1.31$, $\varepsilon = 0.30$.

and noting that $a - 1 > 0$ for the full range, we have to consider the average of the Lyapunov exponent given as

$$\begin{aligned} \Lambda_\infty &= \frac{1}{2} \int_0^1 \ln(4(a_0 - 1 + \varepsilon \sin(2\pi\theta))) d\theta \\ &= \frac{1}{2} \ln(2(a_0 - 1 + \sqrt{(a_0 - 1)^2 - \varepsilon^2})) \end{aligned} \quad (47)$$

which for $a_0 = 1.31$, $\varepsilon = 0.3$ gives $\Lambda_\infty \approx -0.12666931$. The integrand is shown in Figure 7. For the skew product, assuming $\alpha \notin \mathbb{Q}$ and sufficiently small, the two curves which form the attractor, as will be proved later, are very close to the curves $x_1(a)$, $x_2(a)$ of the frozen system. Figure 8 displays the lower one. Also the Lyapunov exponent of the driven map with $\alpha = g/N$, $N = 200$, computed using 10^5 iterates after a transient also of 10^5 iterates is $\Lambda_{200} \approx -0.12680$. Using other values of N , like 100, 400, 800, 1600 the respective values Λ_N obtained are -0.12725 , -0.12670 , -0.126696 , -0.126689 , tending to the limit Λ_∞ .

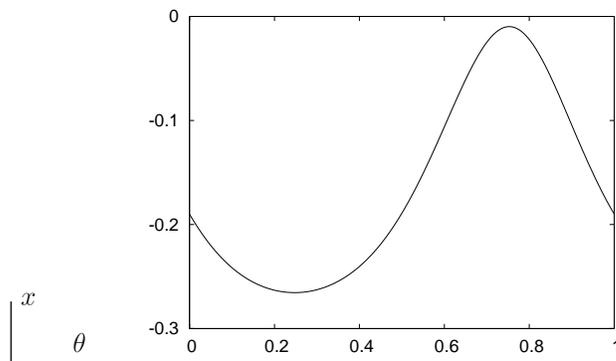


Figure 8. The lower part of the attractor, the graph of $x_1(a(\theta))$, for the parameter values: $a_0 = 1.31$, $\varepsilon = 0.30$.

The numerical difficulties are easy to understand. To compute the Lyapunov exponents, starting at a point x_0 and an initial vector $v_0 = 1$ and setting $S_0 = 0$,

we compute recurrently

$$\begin{aligned}\hat{v}_{j+1} &= DT_a(x_j)(v_j), & x_{j+1} &= T_a(x_j), & n_{j+1} &= |\hat{v}_{j+1}|, & v_{j+1} &= \hat{v}_{j+1}/n_{j+1}, \\ S_{j+1} &= S_j + \log(n_{j+1}).\end{aligned}$$

The values S_j are denoted as Lyapunov sums and the average slope as a function of j (if it exists) gives the Lyapunov exponent Λ . For details and generalisations of this approach, or different alternatives see, e.g., [20], [15] and [18] and references therein.

Even when a Lyapunov exponent is negative it can happen that partial sums have strong oscillations. Given the values of $S_j, j = 0, \dots, k$ let $(S_k)_{\min}$ be the minimum of these values and introduce $O_k = S_k - (S_k)_{\min}$. We define the maximal oscillation of the Lyapunov sums as $OS = \max\{O_k\}$. The Figure 9 shows the behaviour of S_j for $\alpha = g/200$ and also some of the initial oscillations for $\alpha = g/1600$. A non-rigorous computation of OS for $N = 100, 200, 400, 800, 1600$ with 10^5 iterates after a transient gives the values 28.845, 56.761, 112.632, 224.379, 447.874, respectively. This implies a loss in the number of decimal digits equal to these values divided by $\ln(10)$. In particular, between 24 and 25 digits for $N = 200$, which explains the misleading calculations seen in Figure 6. For small α the maximal oscillation tends to be

$$\frac{1}{\alpha} \int_{\theta_2-1}^{\theta_1} h(\theta) d\theta, \quad (48)$$

where $h(\theta)$ is the function which appears as integrand in (47) and it is extended by periodicity outside $[0, 1]$ while $\theta_1 = \frac{3}{4} - \frac{1}{2\pi} \cos^{-1}(0.2)$, $\theta_2 = \frac{3}{4} + \frac{1}{2\pi} \cos^{-1}(0.2)$ are the values at which h becomes equal to zero (see Figure 7). The value of the maximal oscillation in (48) is $\approx 0.172660185/\alpha$ for small α , that if $\alpha = g/N$ becomes $\approx 0.27937N$ in good agreement with the previous results.

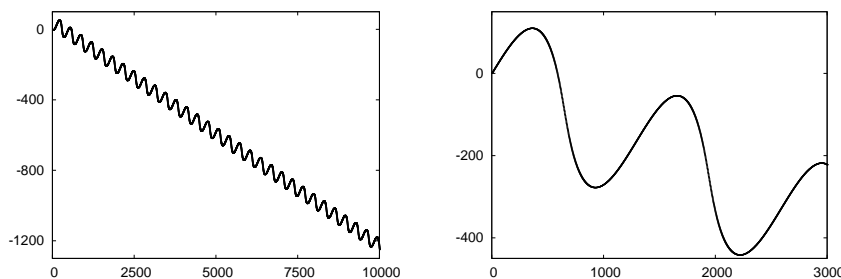


Figure 9. Oscillations of the Lyapunov sums. Left: the Lyapunov sums for $N = 200$. Right: some initial sums for $N = 1600$. Parameter values: $a_0 = 1.31$, $\varepsilon = 0.30$ and $\alpha = g/N$.

Using these ideas one can even predict when we shall observe that the attractor produced by simulations with not enough digits seems to indicate that it is not a period-2 curve. Assume that we do computations with d decimal digits and that in a plot like the one in Figure 6 one can distinguish pixels which are a distance of 10^{-p} . In our example reasonable values of d, p are 16 and 4. This means that from $\theta_2 - 1$, when h

becomes positive, till some unknown θ_d when the “departure” of the iterates from the curve become visible, the factor of amplification of errors is 10^{d-p} or, in logarithmic scale $(d-p)\ln(10)$. This requires

$$\frac{1}{\alpha} \int_{\theta_{2^{-1}}}^{\theta_d} h(\theta) d\theta = (d-p)\ln(10).$$

In our example one finds $\theta_d \approx 0.258$ in good agreement with the observed numerics in Figure 6. In a similar way one can predict the “landing” value θ_l at which the points seen as chaotic in Figure 6 are close enough to the real invariant curves. As the distance from the chaotic points to the true attractor is of the order of 1, the condition is now

$$\frac{1}{\alpha} \int_{\theta_1}^{\theta_l} h(\theta) d\theta = p\ln(10).$$

For the example one obtains $\theta_l \approx 0.629$, again in good agreement with the observed numerics.

This “delayed” observation of the expanding and compressing regimes is similar, but now due to purely numerical reasons, to the delay of bifurcation that can be observed in systems depending on a parameter which has slow dynamics (see [17] and references therein).

5.2. Some limit cases

Now we discuss two limit cases. First one is the case in which $a(\theta)$ covers a wide range. Second one aims at describing the differences between the union of the curves $x_1(a(\theta))$ and $x_2(a(\theta))$ and the true attractor for α small enough.

According to (47) and assuming that for α sufficiently small the attractor is close to the union of the curves $x_{1,2}(a(\theta))$ it is enough to take $a_0 = 1.5 - \delta_1$, $\varepsilon = 0.5 - \delta_1 - \delta_2$ with $0 < \delta_2 \leq \delta_1^2$ to have a negative limit averaged Lyapunov exponent Λ_∞ . If δ_1 is small the values of a almost cover the full range $(1, 2)$. The Figure 10 displays results of the observed behavior using `double precision` for the values $\delta_1 = 0.005$, $\delta_2 = 10^{-6}$, $\alpha = g/60000$. The figure is reminiscent of the “bifurcation diagram” of the logistic map. In fact, a typical way to compute the diagram consists of taking a sample of values of a , do some transient iterates and display some of the next iterates. Now the value of a is changed at every step according to (45) but very slowly, and the transient is discarded. From $\theta = 3/4$ (for which the minimum of $a(\theta)$ is achieved) to $\theta = 5/4 \pmod{1}$ (for which one achieves the maximum) the plot looks like that diagram, except for the bifurcation delays at the period doublings from period 2 to period 4 and successive ones. In the range $\theta \in [1/4, 3/4]$ the reverse situation is seen, but now with much smaller bifurcation delays. The authors do not know if, for the above values of the parameter, the attractor will become close to the union of $x_1(a(\theta))$ and $x_2(a(\theta))$ for computations done with a huge number of digits.

To look for the expression of the attractor as the union of two smooth curves, assuming it is of that type, we restrict our attention to the lower part of it, close to $x_1(a(\theta))$ as given in (46). In principle it is convenient to work with T^2 but, as the

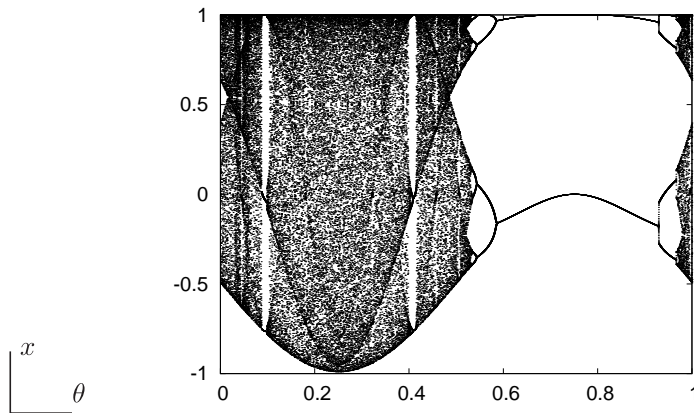


Figure 10. Simulations in double precision for values of a_0, ε such that $a(\theta)$ almost covers the range $(1, 2)$ and α very small. See the text for the numerical values used.

eigenvalues of T^2 along the points of period 2 are negative, we prefer to work with T^4 . We look for the attractor as the graph of a function expanded in powers of α

$$G(\theta) = G_0(\theta) + \alpha G_1(\theta) + \alpha^2 G_2(\theta) + \dots, \quad (49)$$

where $G_0(\theta) = x_1(a(\theta))$ is the zeroth order approximation. The map $T^4(\theta, G(\theta))$ is $\mathcal{O}(\alpha)$ close to the identity. Hence, it can be approximated by a smooth flow (see [1] for proofs, an example of application and additional references, as well as [16] for general results) and the curve we are looking for is a periodic solution of this flow. But we shall proceed by imposing directly the invariance condition.

Starting at a point of the form $(\theta, G(\theta))$ and doing four iterations using the values $a(\theta), a(\theta + \alpha), a(\theta + 2\alpha), a(\theta + 3\alpha)$ we should have

$$T^4(\theta, G(\theta)) - (\theta + 4\alpha, G(\theta + 4\alpha)) = 0. \quad (50)$$

Given values of a_0, ε it is a cumbersome but elementary task to obtain in a recurrent way the expressions of G_1, G_2, \dots from (50). It is essential to reduce the dependence in $G_0(\theta)$, using the equation satisfied by $x_1(a)$, to decrease the order of the powers of G_0 which appear to just the first one. We note also that in the computation of all the terms G_j there appears $16a^2 - 32a + 15 = (4a - 5)(4a - 3)$ in the denominator, which cancels for $a = 5/4$, but a careful examination allows to show that the factor $4a - 5$ is also present in the numerator.

In this way one obtains

$$G_1(\theta) = \frac{3 - 2a - (8a - 9)/\sqrt{4a - 3}}{2a^2(4a - 3)} 2\pi\varepsilon \cos(2\pi\theta), \quad (51)$$

where a stands for $a(\theta)$ as introduced in (45).

The computation of G_2 is much more involved. The simplest expression is given as a rational function depending on $a(\theta), G_0(\theta), G_1(\theta)$ and up to the second derivatives of these functions with respect to θ . Instead, Figure 11 displays the graph of G_1 and

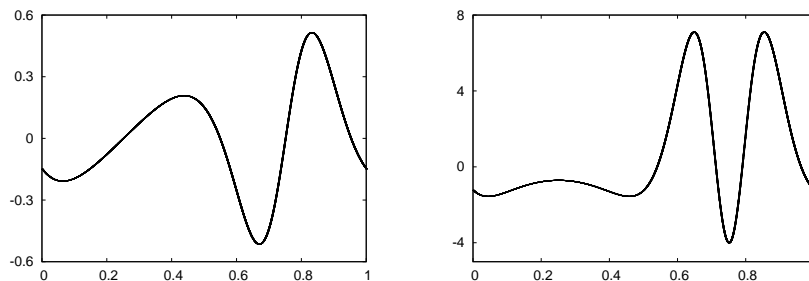


Figure 11. Graphs of $G_1(\theta)$ (left) and $G_2(\theta)$ (right) for $a_0 = 1.31$, $\varepsilon = 0.30$.

G_2 for $a_0 = 1.31$, $\varepsilon = 0.30$. The graph of $G_0(\varepsilon)$ is very close to the attractor shown in Figure 8.

To see tiny details on the attractor Figure 12 displays the differences between the lower part of the attractor, computed with enough digits, and the approximation in (49) up to order 2 in α .

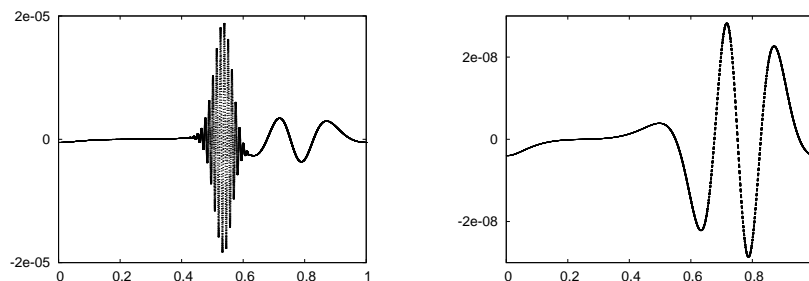


Figure 12. Differences between the attractor and the second order approximation for $a_0 = 1.31$, $\varepsilon = 0.30$ and $\alpha = g/N$. Left: $N = 200$. Right: $N = 1000$.

The left part shows tiny oscillations which were not visible in Figure 8. They reach a maximum at the value $\theta = \theta_1$ for which $h(\theta)$ in (48) changes from positive to negative. As one can expect the shape of these oscillations is a bump function multiplied by a periodic function (close to a sinus) with period 4α . A similar behaviour is observed for many other values of a_0, ε and α . When the oscillations start at a larger distance from θ_1 they can amplify in such a way that the attractor is no longer the union of the two curves. One can suspect that it becomes a non-chaotic strange attractor (see, e.g., [10], [11] and [13]). In contrast, with the same values of a_0, ε but for $N = 1000$ the oscillations are not observed and the very small differences in the plot on the right hand side of Figure 12 are mainly due to the third order term in (49).

5.3. Computer assisted proof of existence of invariant curves

In this section we apply our method from Sections 3 and 5.3.1 to prove that for parameters $a_0 = 1.31$, $\varepsilon = 0.3$ and $\alpha = \frac{g}{200}$, with $g = \frac{\sqrt{5}-1}{2}$ the map T has an invariant

curve.

Around a neighbourhood of the numerical guess for the attractor, the map T^2 is locally invertible. This is due to the fact that our curve is separated from the x -axis. For our proof we consider

$$f = T^{-2}.$$

The attractor is first computed (non-rigorously) by iterating T forwards in time. We then choose a set \mathcal{V} around the attractor (see Figure 13). For most θ the set is a 0.001 radius neighbourhood of the attractor. Close to the angle $\theta = \frac{3}{4}$ we choose \mathcal{V} to be tighter, so that we are sure that it lies within the domain of f (see Figure 13). Our aim is to prove that inside of \mathcal{V} we have an invariant normally hyperbolic curve of f .

The map f is not uniformly expanding in the x direction. Over one part of the set \mathcal{V} the map f is strongly expanding, elsewhere it is contracting. The expansion region lies between two dashed lines on Figure 13. On this set we place ch-sets N_5, \dots, N_{280} of width $\frac{\alpha}{2}$, starting with N_5 on the left and finishing with N_{280} on the right. To the left of them we position additional four ch-sets N_1, \dots, N_4 , also of width $\frac{\alpha}{2}$ (see Figure 13). These lie between two small black lines which point towards the θ -axis in Figure 13 (see also Figure 15). The θ projection of N_i , for $i = 1, \dots, 280$, is $[\theta_0 + (i - 1)\frac{\alpha}{2}, \theta_0 + i\frac{\alpha}{2}]$, where $\theta_0 = \frac{53}{100}$. We shall use a notation

$$U_{k,l} = \bigcup_{i=k}^l N_i.$$

Our ch-sets are parallelograms. The coordinate x is globally expanding for f and coordinate θ is normal (our map does not possess a globally contracting coordinate y). The exits sets N_i^- for the ch-sets are the top and bottom edges of the parallelograms. The map f moves the ch-sets to the left. Since the width of the ch-sets is $\frac{\alpha}{2}$, for $k \in 5, \dots, 280$ we have

$$\pi_\theta f(N_k) \subset \pi_\theta N_{k-4}.$$

In Section 5.3.1 we shall show that (see Figures 14–15)

$$N_k \xrightarrow{f} N_{k-4} \quad \text{for } k \in \{5, \dots, 280\}, \quad (52)$$

and also that (see Figure 14)

$$N_k \xrightarrow{f^{128}} U_{k+135, k+136} \quad \text{for } k \in \{1, \dots, 4\}.$$

In Section 5.3.2 we show how to verify cone conditions. In Section 5.3.3 we briefly describe the tools that were used to conduct the proof.

5.3.1. Verification of covering conditions To describe how covering conditions are verified we start with a seemingly unrelated discussion. Consider a polynomial $p : [0, r] \rightarrow \mathbb{R}$ of degree n

$$p(\theta) = \sum_{j=0}^n a_j \theta^j,$$

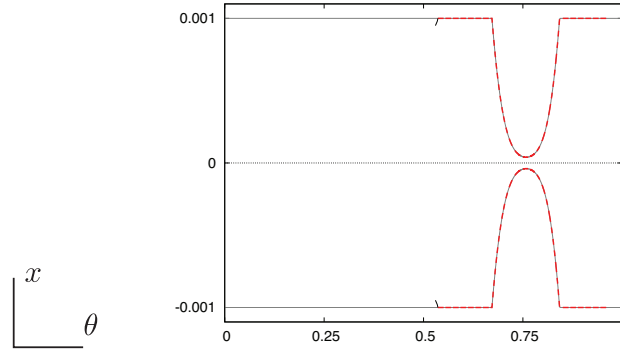


Figure 13. The set \mathcal{V} (between two outer lines), positioning of the ch-sets N_5, \dots, N_{280} (between two dashed lines), and ch-sets N_1, \dots, N_4 (between two very small black lines pointing towards the θ -axis, on the left of N_5, \dots, N_{280}), all plotted relative to the attractor (on the θ -axis).

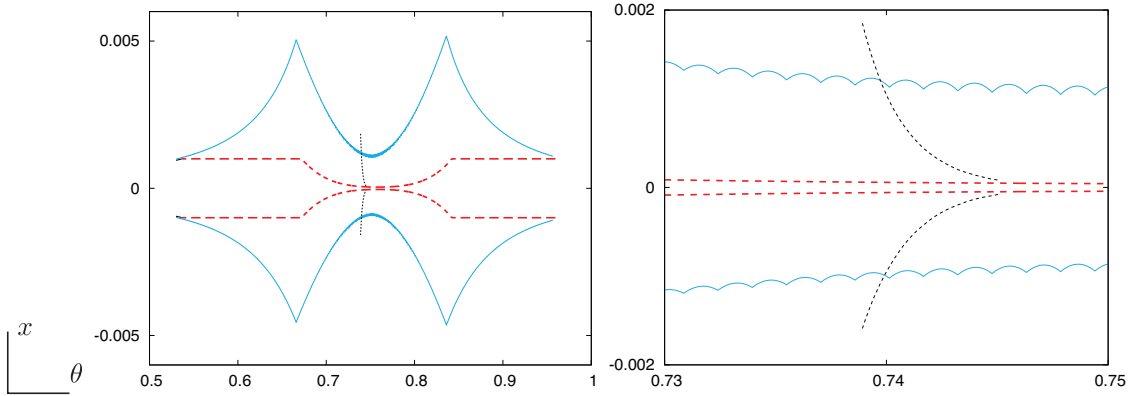


Figure 14. Left: The ch-sets: N_5^-, \dots, N_{280}^- (two long dashed lines; red for colour plots online), N_1^-, \dots, N_4^- (two very short black lines left of N_5^-, \dots, N_{280}^-) plotted relative to the attractor, together with $f(N_5^-), \dots, f(N_{280}^-)$ (two long outer curves; blue for colour plots online) and $f^{128}(N_1^-), \dots, f^{128}(N_4^-)$ (two short dashed curves). Right: Magnification close to $f^{128}(N_1^-), \dots, f^{128}(N_4^-)$.

and a function $g : \mathbb{R} \rightarrow \mathbb{R}$. Using Taylor expansion and defining two polynomials \bar{p} and \underline{p} , of degree n

$$\bar{p}(\theta) = g \circ p(0) + \sum_{j=1}^{n-1} \left(\frac{1}{j!} \frac{d^j (g \circ p)}{d\theta^j}(0) \right) \theta^j \quad (53)$$

$$+ \frac{1}{n!} \left(\frac{d^n (g \circ p)}{d\theta^n}(0) + \frac{1}{n+1} \sup_{v,w \in [0,r]} \frac{d^{n+1} (g \circ p)}{d\theta^{n+1}}(v)w \right) \theta^n,$$

$$\underline{p}(\theta) = g \circ p(0) + \sum_{j=1}^{n-1} \left(\frac{1}{j!} \frac{d^j (g \circ p)}{d\theta^j}(0) \right) \theta^j \quad (54)$$

$$+ \frac{1}{n!} \left(\frac{d^n (g \circ p)}{d\theta^n}(0) + \frac{1}{n+1} \inf_{v,w \in [0,r]} \frac{d^{n+1} (g \circ p)}{d\theta^{n+1}}(v)w \right) \theta^n,$$

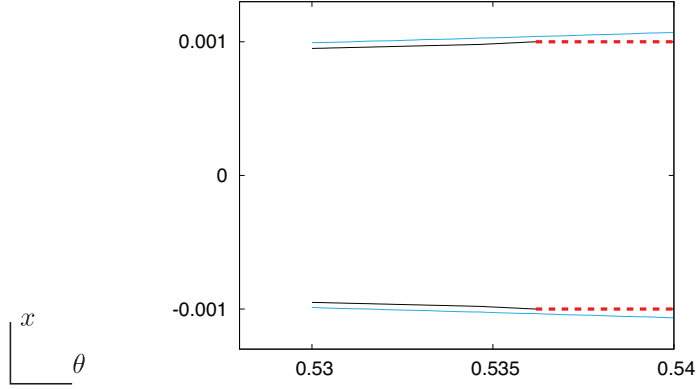


Figure 15. Closeup of the covering $N_i \xrightarrow{f} N_{i-4}$ for $i = 5, 6, 7, 8$ (plotted relative to the attractor). The sets $f(N_5^-), \dots, f(N_8^-)$ are the two outer lines (blue for colour plots online), and the sets N_1^-, \dots, N_4^- are the two inner lines, lying left to the dashed line.

for any $\theta \in [0, r]$ we have

$$\underline{p}(\theta) \leq g(p(\theta)) \leq \bar{p}(\theta). \quad (55)$$

For any $i = 1, \dots, 280$, the exit set N_i^- consists of two lines and can be expressed using two polynomials (in fact these are affine functions) $p_i^u, p_i^d : [0, \frac{\alpha}{2}] \rightarrow \mathbb{R}$, $p_i^d(\theta) = a_{i,0}^d + a_{i,1}^d \theta$, $p_i^u(\theta) = a_{i,0}^u + a_{i,1}^u \theta$ and a point $q_i \in [0, 1)$,

$$\begin{aligned} N_i^- &= N_d^- \cup N_u^-, \\ N_{i,d}^- &= \{(p_i^d(\theta), q_i + \theta) | \theta \in [0, \frac{\alpha}{2}]\}, \\ N_{i,u}^- &= \{(p_i^u(\theta), q_i + \theta) | \theta \in [0, \frac{\alpha}{2}]\}, \\ p_i^d(\theta) &< p_i^u(\theta) \quad \text{for } \theta \in [0, \frac{\alpha}{2}]. \end{aligned}$$

We will now show how to construct a ch-set M such that

$$N_i \xrightarrow{f} M. \quad (56)$$

We first verify that for any point $(\theta, x) \in N_i$ we have $\frac{\partial f}{\partial x}(x, \theta) < 0$. We then take

$$g^u(\theta) := f(q_i + \theta, p_i^d(\theta)), \quad g^d(\theta) := f(q_i + \theta, p_i^u(\theta)), \quad (57)$$

and construct $p^u(\theta) = \bar{p}(\theta)$ using (53) and $p^d(\theta) = \underline{p}(\theta)$ using (54), taking g as functions g^u and g^d respectively. Formula (55) guarantees that $f(N_{i,d}^-)$ lies above the graph of $p^u(\theta)$ and that $f(N_{i,u}^-)$ lies below the graph of $p^d(\theta)$. If we now set

$$\begin{aligned} M^- &= M_d^- \cup M_u^-, \\ M_d^- &= \{(p^d(\theta), q_i - 2\alpha + \theta) | \theta \in [0, \frac{\alpha}{2}]\}, \\ M_u^- &= \{(p^u(\theta), q_i - 2\alpha + \theta) | \theta \in [0, \frac{\alpha}{2}]\}, \end{aligned} \quad (58)$$

and take M to be the set of points between M_d^- and M_u^- then (56) holds.

For $i = 5, \dots, 280$, after applying the above procedure to obtain M which is covered by N_i , we compute bounds on the images of sets

$$p^u \left(\left[\frac{j\alpha}{100}, \frac{(j+1)\alpha}{100} \right] \right), \quad p^d \left(\left[\frac{j\alpha}{100}, \frac{(j+1)\alpha}{100} \right] \right) \quad \text{for } j = 0, \dots, 49, \quad (59)$$

to verify that we have (52) (subdividing $[0, \frac{\alpha}{2}]$ into fifty intervals turns out to be sufficient for all $i \in \{5, \dots, 280\}$).

For $i = 1, \dots, 4$ we need to iterate the procedure (58) many times to obtain a sequence of covering relations

$$N_i \xrightarrow{f} M_{i,1} \xrightarrow{f} M_{i,2} \xrightarrow{f} \dots \xrightarrow{f} M_{i,127} \xrightarrow{f} U_{i+135,i+136}.$$

During our construction we make sure that all sets M_k for $k \in \{1, \dots, 127\}$ lie in \mathcal{V} , which readily holds since the sets are very strongly contracted. Each covering $M_{i,k} \xrightarrow{f} M_{i,k+1}$ holds by construction. Verifying that $M_{i,127} \xrightarrow{f} U_{i+135,i+136}$ is done analogously to (59).

In our computer assisted proof we take the degrees of polynomials for the edges of the sets $M_{i,k}$ as sixteen, which means that we need compute derivatives of the map up to order seventeen. We refer to this as making “ C^{17} computations”. Let us note that computationally this is not as heavy as might seem, since the C^{17} computations are performed for one dimensional functions $g^u(\theta)$ and $g^d(\theta)$ (see (57)). The reduction of dimension truly pays off, since the difference between C^{17} computations in one and two dimensions is substantial.

The estimates obtained by us are very accurate. In Figure 16 we give a plot of the curves $M_{i,128}^-$, for $i = 1, \dots, 4$, and compare them with points from the exit sets of N_i , for $i = 1, \dots, 4$, iterated non-rigorously with high precision computation (depicted with crosses). The curve $M_{i,128,u}^-$ lies below the upper points and the curve $M_{i,128,d}^-$ lies above the lower points, as they should, but they are so close that it is impossible to distinguish this by looking at the plot. The right hand side of Figure 16 shows the difference of the rigorous bound and non-rigorous computation. They turn out to be very close.

Remark 26. Taking 128 iterates of the map turns out to be just the right number for the chosen ch-sets. If we choose less, then we will not obtain the covering. After the 128-th iterate the sets fall out of the domain of f , and it is impossible to take further iterates without ”trimming” them (see Remark 16).

Remark 27. The high order computations and multi-precision in current approach seem essential. The sets $M_{i,k}$ constructed with our procedure are very strongly contracted. The distance between the two curves of $M_{i,k}^-$ at the tightest spot is of order 1.125×10^{-25} , which is extremely thin when compared to the width of the curves $\frac{\alpha}{2} \approx 1.545 \times 10^{-3}$; and yet, with our multi-precision C^{17} approach, with little effort we are able to rigorously keep them apart. Any standard approach, such as performing C^0 computations on sets or careful linearization with C^1 techniques through local coordinates, is likely to fail.

Remark 28. We believe that using a “parallel shooting” type approach it should be possible to conduct the proof using **double precision** and C^r computations for smaller values of r (for this we would need an good a priori guess for the position of the

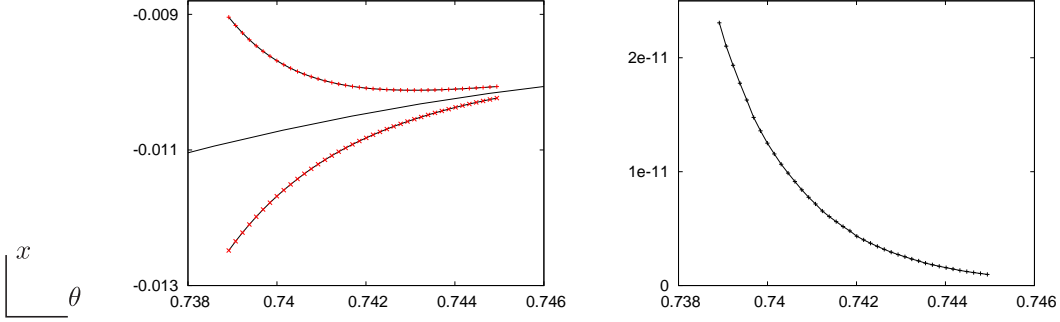


Figure 16. Left: Rigorous bound on the curves $M_{i,128}^-$, for $i = 1, \dots, 4$ (lower and upper curves), together with non-rigorous computations using multi-precision (crosses). The curve in the middle is the attractor. Right: The difference between rigorous bounds and non-rigorous computations.

curve). Such approach could produce a rigorous-computer-assisted proof using **double precision** of an invariant a curve, which is not detectable numerically with **double** computations. This shall be a subject of forthcoming work.

5.3.2. Verification of cone conditions To verify cone conditions let us first rescale our coordinates by

$$\gamma_\beta(\theta, x) = (\beta\theta, x).$$

Taking β sufficiently large, choosing sufficiently many points $\lambda_i \in [0, \beta)$ and taking $h_i := \frac{1}{2}(c^u(\lambda_i) - c^d(\lambda_i))$, $q_i := (\lambda_i, c^d(\lambda_i) + h_i)$ and $V_i := \mathcal{V} \cap ([\lambda_i - h_i, \lambda_i + h_i] \times \mathbb{R})$ we can construct local maps

$$\tilde{\eta}_i : V_i \rightarrow B_c \times B_u,$$

for which $\tilde{\eta}_i(V_i \cap c^u) = B_c \times \{1\}$, $\tilde{\eta}_i(V_i \cap c^d) = B_c \times \{-1\}$ and which are arbitrarily close to a linear map $q \rightarrow \frac{1}{h_i}(q - q_i)$. In these local coordinates, by taking sufficiently large β , we have the following bound on derivatives of local maps (assuming that we choose i, j and p such that $p \in \text{dom}(f_{ij}) \neq \emptyset$)

$$\begin{aligned} Df_{ij} &= D(\tilde{\eta}_i \circ \gamma_\beta \circ f \circ \gamma_\beta^{-1} \circ \tilde{\eta}_j^{-1})(p) \\ &\approx \begin{pmatrix} \frac{1}{h_i} & 0 \\ 0 & \frac{1}{h_i} \end{pmatrix} \begin{pmatrix} \beta & 0 \\ 0 & 1 \end{pmatrix} \begin{pmatrix} \frac{df_1}{d\theta}(\gamma_\beta^{-1}(\tilde{\eta}_j^{-1}(p))) & 0 \\ \frac{df_2}{d\theta}(\gamma_\beta^{-1}(\tilde{\eta}_j^{-1}(p))) & \frac{df_2}{dx}(\gamma_\beta^{-1}(\tilde{\eta}_j^{-1}(p))) \end{pmatrix} \\ &\begin{pmatrix} \beta^{-1} & 0 \\ 0 & 1 \end{pmatrix} \begin{pmatrix} h_j & 0 \\ 0 & h_j \end{pmatrix} \\ &= \frac{h_j}{h_i} \begin{pmatrix} \frac{df_1}{d\theta}(\gamma_\beta^{-1}(\tilde{\eta}_j^{-1}(p))) & 0 \\ \frac{1}{\beta} \frac{df_2}{d\theta}(\gamma_\beta^{-1}(\tilde{\eta}_j^{-1}(p))) & \frac{df_2}{dx}(\gamma_\beta^{-1}(\tilde{\eta}_j^{-1}(p))) \end{pmatrix}, \end{aligned}$$

which in turn is arbitrarily close to $\frac{h_j}{h_i} \text{diag}(\frac{df_1}{d\theta}, \frac{df_2}{dx})$. This means that by using the artificial rescaling γ_β (without the actual need to apply it in practice for our computer assisted

proof), we can divide the region \mathcal{V} into a finite number of sets U_1, \dots, U_N ($\mathcal{V} \subset \bigcup_{i=1}^N U_i$), and verify cone conditions using interval matrices $\text{diag}([\frac{df_1}{d\theta}(U_i)], [\frac{df_2}{dx}(U_i)])$ and applying Lemma 18. For our proof we take $\gamma_0 = (a, b) = (1, -1)$, which means that the quadratic form for our cones is simply

$$Q_{\gamma_0}(\theta, x) = x^2 - \theta^2.$$

If we take $\gamma_1 = ((1 - \varepsilon), 1)$ for any small parameter $\varepsilon > 0$ then by choosing sufficiently large β Assumption 7 is satisfied (since any switch to new coordinates is arbitrarily close to identity). This means that we can take $\gamma_1 = \gamma_0$, provided that all the inequalities in our verification of cone conditions in the computer assisted proof are strict.

5.3.3. Tools used for the proof The source code for the proof is available at the web page of MC (<http://wms.mat.agh.edu.pl/~mcapinsk/papers.html>) and also on the Nonlinearity depositories. It has been conducted with the use of the CAPD library (<http://capd.ii.uj.edu.pl>) developed by the Computer Assisted Proofs in Dynamics group. We have used the multi-precision version of the library running at 128 mantissa bits accuracy (which is approximately equivalent to tracking 40 digits). The C^{17} computations have been performed with assistance of the Flexible Automatic Differentiation Package FADBAD++ (www.fadbad.com). The proof took 36 seconds running on a 2.67 GHz laptop with 4GB of RAM.

6. Final comments

In this paper we have presented a version of a normally hyperbolic invariant manifold theorem, which can be applied for rigorous-computer-assisted proofs. We have successfully applied our method to an example in which standard double precision simulations brake down and produce false results. This demonstrates the strength of our method, that it can handle numerically difficult cases. It needs to be noted that to apply our method we have used multiple precision for our computer assisted computations. For our proof we also needed to apply a high order method which relied on C^{17} computations. We believe that it should be possible to devise a similar in spirit method, which would give proofs without multiple precision and using C^r computations only for a smaller value of r . This will be the subject of our future work.

7. Acknowledgements

We would like to thank Tomasz Kapela for his assistance and comments regarding the implementation of multi-precision computations in the CAPD library. Our special thanks goes to Daniel Wilczak for his suggestions, frequent discussions and for his assistance with implementation of higher order computations in the CAPD library. Finally, we thank Rafael de la Llave for reading our work and for his valuable comments and corrections.

The research of MC has been supported by the Polish State Ministry of Science and Information Technology grant N201 543238. The research of CS has been supported by grants MTM2006-05849/Consolider (Spain), and CIRIT 2008SGR-67 (Catalonia). The computing facilities of the Dynamical Systems group at the University of Barcelona have been widely used.

References

- [1] H. Broer, R. Roussarie, C. Simó, *Invariant circles in the Bogdanov-Takens bifurcation for diffeomorphisms*, Ergod. Th. & Dynam. Sys. **16** (1996), 1147–1172.
- [2] H. Broer, C. Simó, R. Vitolo, *Chaos and quasi-periodicity in diffeomorphisms of the solid torus*, DCDS B **14** (2010), 871–905.
- [3] M. J. Capiński, *Covering Relations and the Existence of Topologically Normally Hyperbolic Invariant Sets*, Discrete and Continuous Dynamical Systems A. Vol. 23, N. 3, (March 2009), pp 705-725
- [4] M. J. Capiński, P. Roldán, *Existence of a Center Manifold in a Practical Domain around L_1 in the Restricted Three Body Problem*, SIAM J. Appl. Dyn. Syst. **11**, pp. 285-318
- [5] M. J. Capiński P. Zgliczyński, *Cone Conditions and Covering Relations for Normally Hyperbolic Invariant Manifolds*, preprint
- [6] M. J. Capiński and P. Zgliczyński, *Covering Relations and Non-autonomous Perturbations of ODEs*, Discrete Contin. Dyn. Syst. Ser. A, **14**, 281–293 (2006).
- [7] Z. Galias, *Positive topological entropy of Chua’s circuit: A computer assisted proof*. Int. J. Bifurcation and Chaos, **7**(2):331-349, 1997.
- [8] Z. Galias and P. Zgliczyński, *Computer assisted proof of chaos in the Lorenz system*, Physica D, **115**, 1998, 165-188.
- [9] M. Gidea and P. Zgliczyński, *Covering relations for multidimensional dynamical systems*, J. Differential Equations , **202**(2004) 33-58.
- [10] C. Grebogi, E. Ott, S. Pelikan and J. A. Yorke, *Strange attractors that are not chaotic*, Physica D **13** (1984), 261–268.
- [11] À. Haro, C. Simó, *To be or not to be a SNA: That is the question*, preprint available at <http://www.maia.ub.es/dsg/2005/>.
- [12] M. Hirsh, C. Pugh and M. Shub, *Invariant Manifolds, Lecture Notes in Mathematics*, Vol. 583. Springer-Verlag, Berlin-New York, 1977.
- [13] T. Jäger, *On the structure of strange non-chaotic attractors in pinched skew products*, Ergodic Theory and Dynamical Systems **27** (2007), 493–510.
- [14] C. K. R. T. Jones, *Geometric singular perturbation theory*. Dynamical systems (Montecatini Terme, 1994), 44–118, Lecture Notes in Math., 1609, Springer, Berlin, 1995.
- [15] F. Ledrappier, M. Shub, C. Simó, A. Wilkinson, *Random versus deterministic exponents in a rich family of diffeomorphisms*, J. Stat Phys. **113** (2003), 85–149.
- [16] A.I. Neishtadt, *The separation of motions in systems with rapidly rotating phase*, Prikladnaja Matematika i Mekhanika **48** (1984), 133–139.
- [17] A. I. Neishtadt, C. Simó, D. V. Treschev, *On stability loss delay for a periodic trajectory*, in Progress in nonlinear differential equations and their applications, Vol 19, pp. 253–278, Birkhauser-Verlag, Basel, Switzerland, 1995.
- [18] J. Puig, C. Simó, *Resonance tongues in the Quasi-Periodic Hill-Schrödinger Equation with three frequencies*, Regular and Chaotic Dynamics **16** (2011), 62–79.
- [19] T. Sauer, *Computer arithmetic and sensitivity of natural measure*, J. Difference Equ. Appl. **11** (2005), no. 7, 669676.
- [20] C. Simó, *Global Dynamics and Fast Indicators*, in *Global Analysis of Dynamical Systems*, H. W. Broer, B. Krauskopf, G. Vegter, editors, pp. 373–390, IOP Publishing, Bristol, 2001.

- [21] D. Wilczak, *Chaos in the Kuramoto-Sivashinsky equations - a computer assisted proof*, J. Differential Equations 194 (2003), no. 2, 433–459.
- [22] P. Zgliczyński, *Covering relations, cone conditions and stable manifold theorem* J. of Diff. Equations 246 (2009) 1774–1819,